Université Catholique de Louvain
Faculté de Médecine
Département d'Imagerie Médicale

Evaluation of multislice spiral CT for the diagnosis of pulmonary embolism

Emmanuel Coche, MD

Thèse présentée en vue de l'obtention
du grade de Docteur en Sciences Médicales (PhD)
Orientation : Recherche Clinique

Promoteur: Prof. Baudouin Maldague

Avril 2005

Promotor:

Baudouin Maldague, MD
Department of Medical Imaging
Cliniques Universitaires St-Luc
Université Catholique de Louvain

Co-promotor:

John R. Mayo, MD
Department of Health and sciences
Vancouver General Hospital
British Columbia University
Vancouver, BC, Canada

Jury:

Catherine Beigelman-Aubry, MD
Department of Radiology
Hôpital Pitié-Salpétrière
Paris, France

François Jamar, MD, PhD
Department of Nuclear Medicine
Cliniques Universitaires St-Luc
Université Catholique de Louvain

Marc Reynaert, MD
Emergency and Critical Care Medicine
Cliniques Universitaires St-Luc
Université Catholique de Louvain

Daniel Rodenstein, MD, PhD
Department of Pneumology
Cliniques Universitaires St-Luc
Université Catholique de Louvain

Stefaan Vynckier, PhD
Department of Radiotherapy
Cliniques Universitaires St-Luc
Université Catholique de Louvain

Lorsque les sciences dévoilent les secrets de la nature, ce que celle-ci perd de mystérieux, elle le gagne en merveilleux.

When science unveils nature's secrets, what is lost in mystery is gained in wonder.

Paul Carvel

Queen Charlotte's Island, British Columbia, Canada, Summer 1997

A Caroline et mes enfants
To Caroline and my children

A mes parents
To my parents

Acknowledgements:

This thesis is the end-result of several years work spent both abroad then in St-Luc University Hospital.

I particularly wish to thank **Prof. Baudouin Maldague**, the promotor of this thesis, who encouraged me and gave me his support towards the Belgian and foreign academic authorities during all that time.

I am also most indebted to **Prof. Philippe Grenier** and **Dr. Catherine Beigelman-Aubry** who initiated me to clinical research in thoracic imaging in 1994 at the Pitié-Salpétrière Hospital in Paris. The clinical and human experience I acquired during my visiting time there is unforgettable.

I am very grateful to **Prof. Patrice Bret** for teaching me the basics of computer science and experimental data exploitation during my "clinical and research fellowship" spent in the years 1994-1996 at the Montreal General Hospital.

I also extend my thanks to **Prof. Nestor Müller** who welcomed me in his Department of Medical Imaging at Vancouver General Hospital in 1996-1997. **Prof. John Mayo**, initiator of this thesis, and **Mrs Lisa Baile** extensively taught me how to conduct and supervise the animal experiments detailed at the beginning of this work. I take this opportunity to thank them for their precious collaboration.

This thesis could never have been finished without the support and advice of **Prof. Jacques Melin, Prof. Vincent Grégoire** and that of my colleagues of the Department of Medical Imaging, more specifically **Doctors** and **Professors Louis Goncette**, **Etienne Danse**, **André Noël Dardenne**, **Bernard Van Beers** and **Laurence Annet**, who allowed me to escape from my clinical activity from time to time during the past academic year, for which I am most grateful.

Neither could this work have been accomplished without the continuous collaboration and exchange of ideas with clinical doctors, such as in particular **Dr Franck Verschuren, Prof. Francis Zech, Prof. Philippe Hainaut and Prof. Daniel Rodenstein.** I thank all the **co-authors** of the papers cited in the present thesis and all the **members of the jury for** their attendance and constructive criticism. I am also very grateful to **Mrs Octave-Prignot** and **Prof. Stefaan Vynckier**, who helped me with the realization and dosimetric analysis of the CT scans. I thank also **Mr Alain Vlassenbroek** and **Philips Medical Systems** for their successful partnership.

All the **nursing staff and technicians** of the CT unit who helped me without tiring in order to achieve high quality examinations must be warmly remembered and thanked, as do all the **patients** who have undergone radiological examinations under my care during this thesis. I also extend my thanks to **Mrs Françoise Martin** for her precious help in typing this thesis, **Mrs Martine Milecan** for her bibliographic research, and **Dr Claire de Burbure** for her help in proofreading this work.

Finally, this thesis could never have been completed without the huge and constant support and encouragement of my wife **Caroline** and of my children **Adrienne, Maximilienne, Eugénie, Juliette, Théophile** and **Constantin**. I particularly wish to thank them for their patience every time I was away from home or in front of my computer screen during these past few years.

Warm and special thanks to my parents and my father-in-law for always encouraging and supporting me in my various enterprises.

Cette thèse est l'aboutissement d'un travail de plusieurs années passées à l'étranger et ensuite au sein des Cliniques Universitaires St-Luc.

Je tiens à remercier à ce propos le Professeur **Baudouin Maldague**, promoteur de cette thèse, qui m'a encouragé et soutenu auprès des autorités académiques belges et étrangères durant toute cette période.

J'adresse également mes plus vifs remerciements au professeur **Philippe Grenier,** au Docteur **Catherine Beigelman-Aubry** qui m'ont initié à la recherche clinique en imagerie thoracique lors de mon passage en 1994 à l'Hôpital Pitié-Salpétrière (Paris). Je garde de ce stage une expérience clinique et humaine inoubliable.

J'exprime ma reconnaissance au Professeur **Patrice Bret** qui m'a appris les bases de l'informatique et l'exploitation des données expérimentales tout au long de mon « clinical and research fellowship » effectué de 1994-1996 au Montreal General Hospital (Montréal).

J'exprime ma gratitude envers le Professeur **Nestor Müller** qui m'a accueilli en 1996-1997 au sein de son département d'imagerie médicale au Vancouver General Hospital (Vancouver). Le Professeur **John Mayo,** initiateur de cette thèse et Madame **Lisa Baile** m'ont appris énormément dans la conduite et la supervision des expérimentations animales qui ont été menées au début de ce travail. J'en profite également pour les remercier de leur collaboration précieuse.

Cette thèse n'aurait pu être réalisée sans l'appui et les conseils du **Professeur Jacques Melin** et du **Professeur Vincent Grégoire** ainsi que de mes collaborateurs du service d'imagerie médicale et plus spécialement les professeurs et docteurs **Louis Goncette**, **Etienne Danse**, **André Noël Dardenne**, **Bernard Van Beers** et **Laurence Annet** qui m'ont permis de m'échapper partiellement de mon activité clinique durant l'année académique écoulée, je les en remercie vivement.

Ce travail n'aurait pas pu être accompli sans la collaboration continue et les échanges d'idées avec les médecins cliniciens. Je pense plus particulièrement au Docteur **Franck Verschuren,** Professeurs **Francis Zech, Philippe Hainaut** et **Daniel Rodenstein.** Je remercie également tous les collègues qui ont participé à l'élaboration des articles cités dans ma bibliographie personnelle ainsi que tous les **membres de mon jury** pour leur présence et leurs critiques constructives. Je suis également très reconnaissant envers Madame **Octave-Prignot,** le Professeur **Stefaan Vynckier** qui m'ont aidé dans la réalisation et l'analyse dosimétrique du CT. Je remercie également Monsieur **Alain Vlassenbroek** et **Philips Medical Systems** pour leur partenariat fructueux.

Je ne peux oublier l'aide quotidienne des **manipulateurs** et **infirmières** de tomodensitométrie qui m'ont aidé sans relâche pour effectuer des examens de haute qualité, ni la participation de tous les **patients** aux examens radiologiques durant cette thèse. Je remercie vivement Madame **Françoise Martin** pour son aide précieuse dans la dactylographie de cette thèse, Madame **Martine Milecan** pour sa recherche bibliographique et Docteur **Claire de Burbure** pour son aide à la correction linguistique de cet ouvrage.

Enfin, cette thèse n'aurait jamais pu être réalisée sans les encouragements et le soutien important de mon épouse **Caroline** et de mes enfants : **Adrienne, Maximilienne, Eugénie , Juliette, Théophile** et **Constantin**. Je les remercie tout particulièrement pour leur patience envers toutes les heures que j'ai passées ces dernières années en dehors du milieu familial ou en face de mon écran d'ordinateur.

Une tendre pensée va tout naturellement à mes parents et à mon beau-père qui m'ont toujours soutenu et encouragé dans mes différentes démarches.

Table of contents

SUMMARY

Pulmonary embolism (PE) is a severe frequent disease with lack of specific symptoms and represents a major diagnostic challenge. In the past few years, single-slice spiral CT angiography has gained acceptance as a minimally invasive method of evaluating patients with suspicion of PE. The main limitation of single-slice spiral CT resides in the poor detection of sub-segmental or more distal PE. This limited detection is not explained by an insufficient vascular distension during spiral CT acquisition but probably by an insufficient spatial resolution. Moreover, in some situations spiral CT is penalized by pulmonary angiography which is an imperfect gold standard.

Today Multislice CT can acquire 2 up to 64 slices in a single rotation with isotropic resolution. This technique can cover the entire chest in 1-mm slice thickness or less, in one short breath-hold and allows a better analysis of peripheral pulmonary arteries with a better depiction of sub-segmental and peripheral clots. It also reduces or eliminates artefacts produced by patient movement and decreases the x-ray tube heating that can constrain single-slice scanning parameters. Acquisition of the lower extremities can be performed after chest CT, allowing detection of deep vein thrombosis and one stop shopping of the venous thromboembolic disease. The diagnostic accuracy of multislice CT is probably similar or superior to pulmonary angiography with an inferior delivered radiation dose, a better detection of alternative diagnoses and a continuous decrease of contrast medium injected. Last refinements in CT technology opens new frontiers for a functional approach of PE and predict its prognosis.

For all the above-mentioned reasons, it seems obvious that multislice CT will definitively replace pulmonary angiography for diagnostic purposes and will represent a superb tool to better understand the physiopathology of this frequent and potentially life-threatening disorder.

INTRODUCTION

Pulmonary embolism (PE) (fig.1) is a severe frequent disease and one of the leading causes of mortality in hospitalized patients. Deep vein thrombosis (DVT) of the limbs and PE are often associated and constitute the same entity called venous thromboembolic disease. In patients with confirmed PE, the prevalence of detectable residual DVT at the time of an acute PE event is largely unknown. The very few studies in which such data can be found provide discrepant results, with the prevalence of DVT ranging from 13 to 93% (1-4). A study found in 228 consecutive patients with an angiography-proven acute pulmonary embolism and bilateral lower limb venography (5) a high prevalence (82%) of residual DVT. About 50% of patients with confirmed DVT of “either” lower or upper extremities have PE (6-12).

Because of the silent nature of this disease, its highly atypical clinical presentation, and the cost and inconvenience of the standard diagnostic tools, total incidence, prevalence, and mortality rates of venous thromboembolic disease remain elusive, especially in the case of PE. The estimated annual incidence of acute PE is 69 cases per 100 000 persons in the United States (13), which means that more than 175 000 persons develop established PE each year. Prospective studies have documented a 30% to 40% prevalence of PE in patients who have clinical features of suspected PE (14-16). The rate of recurrence after an initial episode of PE has been found to be 8% in patients treated with anticoagulant therapy, but may reach 30% in untreated patients. In the International Cooperative Pulmonary Embolism Registry of 5454 consecutive patients from 52 institutions in seven countries, the 3-month mortality rate was 17.4% (17). In a Japanese registry of 533 patients with PE, the in-hospital mortality rate was 14% (18).

It has been estimated that most deaths occur within the first two hours following the initial event. Therefore, both rapid diagnosis and prompt initiation of the appropriate therapy are crucial for the patients’ prognosis (19).

Dyspnea, chest pain, and cough are the most frequent symptoms whereas tachypnea and tachycardia are the most frequent clinical signs in PE. Electrocardiography might reveal findings that are associated with the diagnosis of PE: S1Q3 pattern, incomplete right bundle branch block and

complete right bundle branch block occur in a small minority of cases. Acute PE impairs the efficient transfer of oxygen and carbon dioxide across the lung. Decreased arterial PO_2 (hypoxemia) and a lower than normal arterial PCO_2 are the most common gas exchange abnormalities.

Previous venous thromboembolism, prolonged immobilization, cancer, recent orthopedic surgery, estrogen therapy, age, travel and coagulation disorders all increase the risk of PE. The search for PE risk factors contributes significantly to its diagnosis. Most studies indicate that 30% of investigated patients ultimately carry the diagnosis of PE. More refined diagnosis algorithms are thus needed to confirm the presence of thromboembolic disease and to allow more efficient use of medical resources. At least two scoring systems, the Wells (20) or Canadian score (table1), and the Wicki (21), or Geneva score have been proposed to quantify the clinician pretest probability. The Canadian score is practical and easily applicable to all patients with suspected PE but it has been shown that only 37% of the physicians noted their pretest probability in the patient's records (22).

Table 1. Canadian (Wells) clinical prediction rule

Item	Points
Clinical signs and symptoms of DVT (minimum of leg swelling and pain with palpation of deep veins)	3
An alternative diagnosis is less likely than PE	3
Heart rate greater than 100	1.5
Immobilization or surgery in the previous 4 weeks	1.5
Previous DVT/PE	1.5
Hemoptysis	1
Malignancy (on treatment, treated in last 6 months or palliative)	1

Low pre-test probability (>2points), intermediate pre-test probability (2-6 points), and high pre-test probability (>6points)

In the past, medical practitioners had several imaging tools to diagnose venous thromboembolism: chest X-ray, ventilation-perfusion scintigraphy, Color Doppler venous ultrasonography, contrast venography, cardiac echocardiography and pulmonary angiography.

A **chest radiograph** is usually the first imaging study performed in patients with suspected PE. This test has limited value to establish or exclude the diagnosis of PE. However, this imaging modality is helpful to exclude diagnoses that may clinically mimic PE.

The Ventilation/Perfusion (V/Q) scan was the initial modality obtained in patients with a suspected diagnosis of PE for a number of years. Although many studies investigated the role of V/Q scan in the evaluation of thromboembolic disease, the Prospective Investigation of Pulmonary Embolism Diagnosis (PIOPED) study (15) provided most useful information regarding the utility of V/Q scan in this setting.

A high-probability scan interpretation is sufficient justification to institute anticoagulation. According to the PIOPED study, most patients with high-probability V/Q scans had angiographic evidence of PE (102/116 definitive studies, or a positive predictive value of 88%) but only 102/251 patients with angiograms that showed thromboembolic disease had high-probability V/Q scans. The sensitivity was therefore only 41%.

A normal perfusion scan effectively excludes the diagnosis of PE. Only 5% of PIOPED patients (5/128) with a normal/near normal scan reading had PE. A normal/near normal scan interpretation carries therefore a sufficiently low prevalence of angiographically proven PE to withhold anticoagulation treatment.

However the number of patients entering the high-probability or near normal/normal V/Q scan reading category is relatively rare. According to the PIOPED study, only 13% of patients had high-probability scans while 14% had near normal/normal probability V/Q scans. By contrast, approximately 70% of the studied population had intermediate or low-probability V/Q scan results. Among patients with intermediate V/Q scans readings, 33% had a PE requiring further angiographic evaluation.

Color Doppler ultrasonography and **contrast venography** represent non-invasive and invasive methods for the objective diagnosis of DVT. Color

Doppler ultrasound can and should be used as a first line alternative to venography, and can usefully be employed for the exclusion of both above- and below-knee deep venous thrombosis (23). Although a normal examination essentially excludes a diagnosis of proximal vein thrombosis, it does not exclude acute PE.

Echocardiography may be used in patients with suspicion of massive PE and usually enables the non-invasive measurement of the pulmonary artery pressure, right ventricular volume and function, which all help in determining the hemodynamic consequences of pulmonary embolus (24).

Transesophageal echocardiography has the additional advantage of directly identifying pulmonary embolism in some patients (25, 26).

Pulmonary angiography has been the gold standard for the diagnosis of PE for decades. Studies have indicated that angiography has probably been underused by referring physicians for the evaluation of suspected PE, mainly because of the perception of significant morbidity and mortality associated with the procedure. Pulmonary angiography has an overall complication rate of 6% (27). Reported Complications were death in 0.5% patients, major nonfatal complications in 1% and less significant or minor in 5% of patients.

Two recent studies have demonstrated that the inter-observer agreement rates for detection of subsegmental PE ranged between only 45 and 66% (28,29). We will see during this thesis that this test is limited for unequivocal diagnosis of peripheral PE and that the status of pulmonary angiography as the standard of reference appears questionable.

During the last decade, interest has developed in the use of **Spiral Computed Tomography (CT)** for the diagnosis of PE. Spiral CT scanning produces volumetric two-dimensional images of the lung by rotating the detector around the patient. Total acquisition time is less than 30 seconds with 5 mm collimation using a single row of detectors. Spiral CT is minimally invasive and can help identify other disorders that may be responsible for the patient's symptoms.

Major progress in CT technology has recently been achieved with the introduction of multislice CT (30). This technique provides a submillimeter resolution in all three spatial dimensions and therefore much more detailed anatomical information in each acquired image. One millimeter-thick slices of

the whole thorax can be acquired in 10 seconds or less. Our institution owns different generations of multislice CT (2 slices, 4 slices and 16 slices CT, and in the near future 40 and 64-slices) and provides an ideal environment for the evaluation of the use of the latest CT technology in the field of thromboembolic disease.

The objectives of this thesis are twofold: first, to understand the limitations of single-slice spiral CT in the detection of subsegmental PE and second, to evaluate the multislice CT technology and its performance to detect acute PE.

2. SPIRAL COMPUTED TOMOGRAPHY IN THE DETECTION OF PULMONARY EMBOLISM

2.1. Assessment of acute PE with single-slice spiral CT (papers 1-2)

Today, single-slice spiral CT is known as an accurate and relatively non invasive method that is often usefully applied to the diagnosis of central and segmental PE.

The first description of using CT technique in the assessment of pulmonary arteries was given by Remy-Jardin et al. in 1992 (31). Images were obtained with a spiral volumetric technique using 5-mm-thick sections, 5-mm/sec table feed with reconstruction of overlapped images within a limited scanning volume of 12 cm from the aortic arch down to the diaphragm. The scanning time was 24 seconds. Contrast material was injected at a rate of 5-7 ml/sec with a concentration of 12% to 30% iodine content and a 5-second scanning delay. Since this original description, many authors (32-38) have modified this technique in accordance to their own equipment specifications and habits.

At contrast-enhanced spiral CT, pulmonary emboli are directly visualized on mediastinal window setting (350-50 Hounsfield Unit) as (a) a complete obstruction of a normal-sized or enlarged pulmonary artery or as (b), non-enhancing intravascular filling defects in pulmonary arteries (Fig.2). With spiral CT, volume data can be acquired without mis-registration of anatomical details, an advantage which initiated the development of 2D and 3D post-processing techniques. Multi-planar reformations (MPRs) allow reconstruction of axial image data in all desired planes. This post-processing technique is often used in routine clinical practice and may help the radiologist to differentiate extravascular structures such as lymph nodes from intravascular clots or emboli (39-41). Maximum-intensity projection (MIP) is another very popular technique for rendering vascular structures. This image is derived by projecting onto an image plane the highest attenuation voxel encountered in a ray through the scan volume. This method provides the best sensitivity in the visualization of small vessels but small emboli may be missed with adjacent hyper attenuating voxels. Shaded surface display (SSD) provides excellent images through choosing proper voxel data and thus excluding irrelevant

structures. This technique may be used to increase our understanding of pulmonary arterial anatomy and detect accessory pulmonary vessels. Volume rendering (VR) is a relatively new technique used for the visualization of the vasculature using all voxel data and maintaining three-dimensional relationships. This model provides some of the advantages of both MIP and SSD. Each voxel is adjusted to different opacity, color and brightness according to each CT value using the opacity function and a color map. This technique offers excellent images of the pulmonary arteries and a synthetic comprehensive view of the thromboembolic disease for the referring clinician (Fig.3).

Several clinical prospective studies have shown the sensitivity and specificity for the detection of acute PE to be approximately 90% in central and segmental vessels (31-38) (Table 2). Diagnostic accuracy decreases when subsegmental arteries are included in the analysis (36-38) with a sensitivity ranging from 45 to 65%.

A recent systematic literature (42) review revealed a wide range of reported sensitivities, only a minority of which exceeded 90%. The combined sensitivities of CT for detecting PE ranged from 66% to 93% and the combined specificities ranged from 89% to 97%. Only one of the reviews reported a combined sensitivity greater than 90%. Another review paper (43) states that use of spiral CT for the diagnosis of PE has not been adequately evaluated. The safety of withholding anticoagulant treatment in patients with negative results on spiral CT is uncertain. Further large prospective studies should be done to evaluate diagnostic accuracy and safety of single-slice spiral CT for diagnosis of suspected PE.

Figure 1

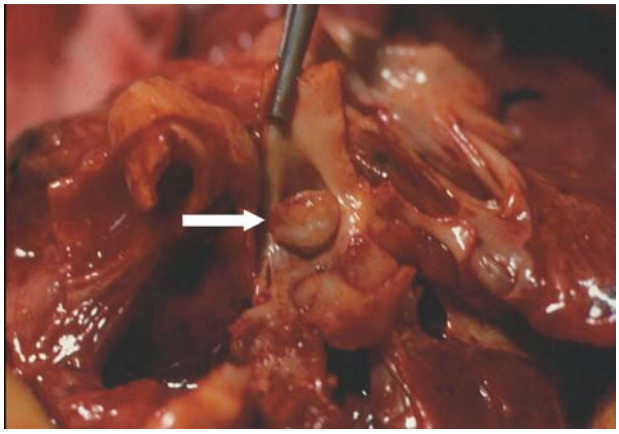

Acute pulmonary thromboembolism is the result of the sudden migration into the pulmonary arteries of clots that mostly have their origin in the lower limb veins. This migrating material may be partially or totally occlusive as shown on this surgical specimen (white arrow) .

Figure 2

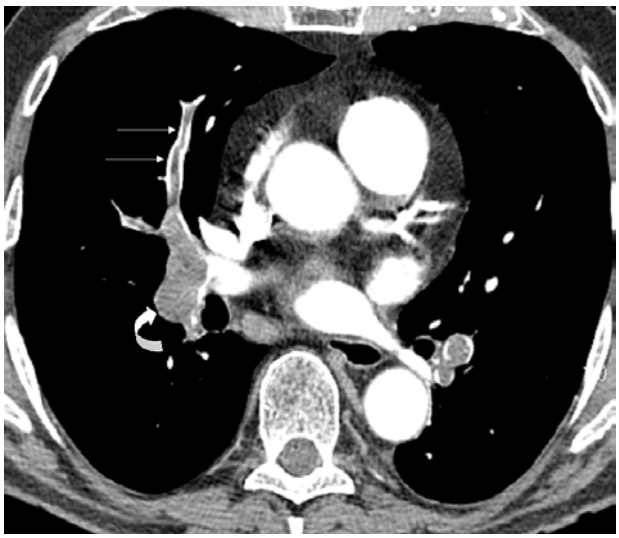

The diagnosis of acute PE on contrast-enhanced CT is based on the presence of partial or complete filling defects. A partial defect is defined as an intravascular central or marginal area of low attenuation surrounded by a variable amount of contrast material (straight arrows). A complete occlusive filling defect is defined as an intraluminal area of low attenuation that occupies the entire arterial section (curved arrow).

Figure 3

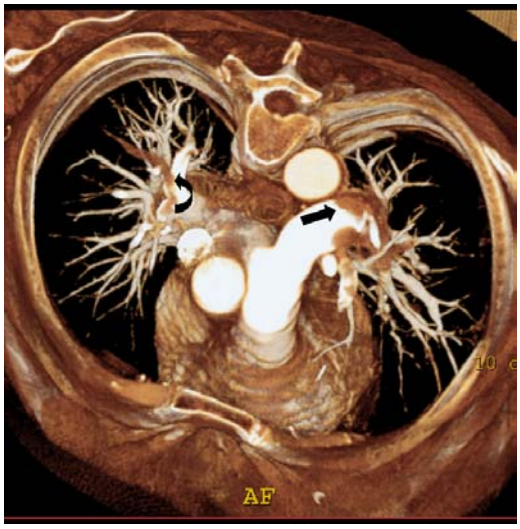

Volume rendering view in a patient with acute PE in left main pulmonary artery (straight arrow) and right upper lobe segmental pulmonary artery (curved arrow). The extent of the thrombotic changes is well seen on this synthetic view.

Figure 4

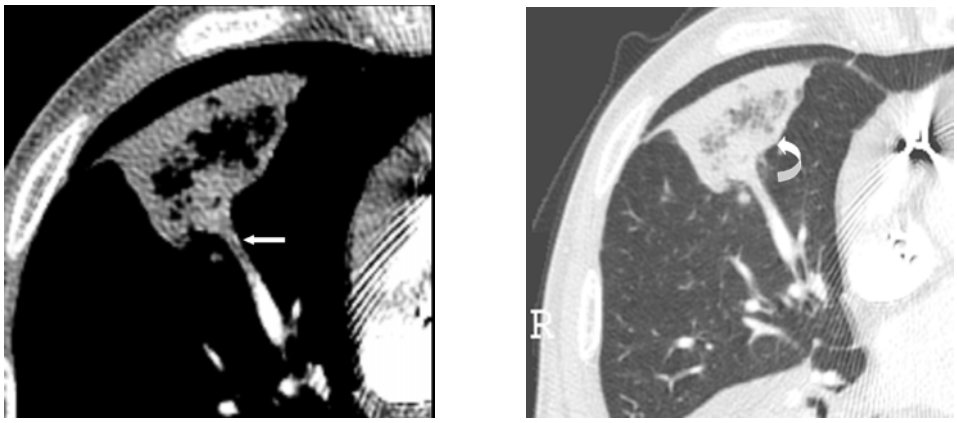

A B

A contrast-enhanced spiral CT in a 72-year-old man with recurrent chest pain and dyspnea. This patient had a previous episode of thromboembolism treated by anticoagulation and inferior cava filter placement. Axial view of thin section CT (soft-tissue window settings (A) and lung window settings (B), 1.3 mm collimation, 0.6 mm interval reconstruction) revealed the inferior pleural-based (minor fissure) wedge-shaped opacity partially aerated in the right middle lobe (curved arrow). The peripheral artery leading to it was thrombosed (straight arrow). The diagnosis of recurrent PE with pulmonary infarction was established.

Table 2. Accuracy of spiral CT in the diagnosis of acute PE

	Single slice CT Protocols						
Study	Year	N	Collimation	Lower anatomical level of interpretation	Sensitivity (%)	Specificity (%)	κ Value
Remy-Jardin et al. (31)	1992	42	5	Segmental	100	96	NA
Remy-Jardin et al. (32)	1996	75	5.3	Segmental	91	78	NA
Van Rossum et al (33)	1996	149	5	Segmental	82-90	93-96	0.77
Mayo et al. (34)	1997	142	3	Segmental	87	95	0.85
Van Rossum et al. (35)	1996	123	5	Segmental	75	90	NA
Teigen et al. (36)	1995	60	6	Subsegmental	65	97	NA
Goodman et al. (37)	1995	20	5	Subsegmental	63	89	NA
Velhamos (38)	2000	22	3	Subsegmental	45	82	NA

Ancillary findings in relationship with PE can also be observed on spiral CT. During our first clinical work (44), we demonstrated in 88 non-consecutive patients that the ancillary signs of wedge-shaped pleural-based consolidation, linear bands, and dilated central or segmental pulmonary arteries were significantly *(P* < .05) associated with PE on enhanced single-slice spiral CT. Identification of these ancillary signs at CT may be useful to direct further investigations when there is suboptimal visualization of central or segmental vessels.

The most common finding in the lung parenchyma of patients with acute PE in our study was wedge-shaped pleural-based consolidation (Fig.4). As in previous studies (45), the sensitivity of this finding for diagnosis of PE was greater at CT (62%) than plain radiography (24%). In contrast to the plain radiographic findings in the Prospective Investigation of Pulmonary Embolism Diagnosis (15), this sign was seen significantly *(P* < .05) more commonly in patients with acute PE in our CT study and was suggestive of pulmonary infarct. A marked lower-lobe predominance was noted for wedge-shaped pleural-based consolidation, in agreement with results of studies on the distribution of this sign on chest radiographs (46) and in agreement with the distribution of pulmonary emboli.

Although the distribution of wedge-shaped pleural-based areas of consolidation correlated with the distribution of segmental emboli, particularly in the right lower lobe, a one-to-one association was not seen. Absence of a precise association was probably due to the limited spatial resolution (particularly in the Z axis) of single-slice spiral CT scanners, which does not allow reliable detection of emboli distal to the segmental level. No significant association (P > .05) was found between PE and detection of non-wedge-shaped consolidation, decreased lung attenuation, or isolated atelectasis on CT scans, as in chest radiographic studies of these findings (46).

Linear bands were seen more frequently in patients with PE (P < .05) than in patients without PE (sensitivity, 46%; specificity, 79%). Owing to their configuration, linear bands are easily detected at CT but are only clearly seen at plain radiography when fortuitously viewed along their long axis. For this reason, the diagnostic value of this finding has, to our knowledge, not been addressed in plain radiographic studies. It has been suggested that linear bands are secondary to previous pulmonary infarction (45), severe infection, or discoid atelectasis. In our study, this finding was more common at the lung bases.

Although pleural effusion was seen in patients with PE (sensitivity, 50%), it was also seen in patients without PE (specificity, 42%), in agreement with the results of previous plain radiographic studies (sensitivity, 35%; specificity, 70%) (46). As in the plain radiographic studies, the presence of pleural effusion was not significantly associated with PE (P > .05).

The CT correlate of the Fleischner sign in plain radiography — an enlargement of central pulmonary arteries — was detected in the left interlobar and right main pulmonary arteries ($P < .05$). Enlargement of segmental pulmonary arteries that contained emboli ($P < .05$) was also identified in this study (46). These results are in agreement with those of a previous study (37), in which segmental pulmonary arteries that contained emboli were frequently larger than adjacent vessels without emboli.

2.2. Limitations of single-slice spiral CT

2.2.1. Limited detection of subsegmental PE

The prevalence of PE limited to subsegmental arteries is variable and varies between 6 and 33% of the patients with PE (15,37,47,48). Quinn and associates (47) reported PE limited to subsegmental pulmonary arteries in 2 out of 20 (10%) patients with PE. Oser et al. (48) showed PE limited to subsegmental or smaller arteries in 23 out of 76 (30%) patients with angiographically diagnosed PE. Goodman and associates (37) showed PE limited to subsegmental pulmonary arteries in 4 out of 11 (36%) patients with angiographically diagnosed PE. Over the past few years, it has been reported that spiral CT was thought to be less accurate than pulmonary angiography (36-38) in the detection of subsegmental emboli. Teigen et al. (36), Goodman et al. (37) and Velmahos (38) reported suboptimal sensitivity of single-slice CT (65, 63% and 45% respectively) when all emboli, including small segmental and subsegmental emboli, were considered.

A question often raised over the past few years concerns the clinical relevance of peripheral emboli in acute PE. Several authors consider that tiny clots originating from calf veins do not require anticoagulation (37,49-51). However, occlusion of a few subsegmental branches perfusing the most "normal" part of the lung parenchyma has been reported to lead to respiratory failure in patients with pre-existing bronchopulmonary disease (31, 46). In our institution we usually initiate anticoagulation therapy in all patients with isolated peripheral PE, as long as there are no contra-indications.

2.2.2. Inconclusive CT examinations

Single-slice spiral CT examinations are considered as inconclusive in approximately 10 to 15% of patients addressed for suspicion of PE (31-38). These technical failures have been observed in patients with severe dyspnea responsible for poor image quality (32, 52). Several factors are responsible for difficulties of interpretation: obliquely oriented arteries, presence of hilar lymph nodes, kinetic and flow-related artifacts, insufficient vascular enhancement (53).

2.2.3. Medical conditions

Detection of PE with spiral CT necessitates the injection of iodinated contrast material. One hundred to one hundred fifty ml of contrast medium containing 300 to 350 mg of Iodine/ml are usually required. No consensus exists (54) concerning the optimal injection protocols for studying pulmonary arteries at spiral CT. Allergy to contrast media (55, 56), renal failure (57, 58), Metformin intake (59) constitute relative contra-indications to perform enhanced spiral CT.

A past medical history of moderate or severe adverse reaction to contrast media is an important risk factor (55). In series of over 330,000 patients analyzed by Katayama et al. (56) there was a six-fold increase in reactions to both ionic and non ionic contrast-media following a previous severe adverse reaction. Asthma is also an important risk factor with a reported six- to ten-fold increase in the risk of a severe reaction in such patients (56). When patients report a previous severe reaction to contrast media, most radiologists try to avoid having to give intravascular contrast media, if at all possible (55). If the examination is considered essential, non-ionic contrast media are the agents of choice based on the evidence in literature that the risk of reacting to them is reduced by a factor of four to five (56). The potential risk of the procedure should be explained to the patient, and the resuscitation team should be present when the contrast medium is given (55).

Risk factors for contrast medium induced nephropathy include diabetes mellitus, advanced age, use of diuretics, hypertension, nephrotoxic

medications, dehydration, multiple myeloma, congestive cardiac failure, previous myocardial infarction and a large dose of contrast material (58). The referring clinician must be involved in identifying patients at risk. A recent serum creatinine level should be obtained in patients with a history of risk factors (58).

Intravascular administration of iodinated contrast media to patients who are receiving Metformin, an oral antidiabetic agent, can result in lactic acidosis (59). However, this rare complication occurs only if the contrast medium causes renal failure and if the patient continues to take Metformin in the presence of renal failure. Because Metformin is excreted primarily by the kidneys, continued intake of Metformin after the onset of renal failure results in a toxic accumulation of this drug and subsequent lactic acidosis. To avoid this complication, Metformin must be withheld after the administration of the contrast agent for 48 hours, during which the contrast-induced renal failure becomes clinically apparent. If renal function is normal at 48 hours, the Metformin can be restarted.

2.3. Why does single-slice spiral CT not detect sub-segmental PE accurately?

2.3.1. A question of vascular distension (paper 3)?

Over the past few years, several studies have stressed that subsegmental pulmonary arteries were not accurately evaluated with spiral CT. Subsegmental vessels, which measure 2-5 mm in diameter, lie at the spatial resolution limits of spiral CT performed with 3-mm collimation (60). These vessels also lie near the spatial resolution limits of digital subtraction pulmonary angiography (61). We hypothesized that the pulmonary arterial injection used in pulmonary angiography might distend these subsegmental vessels, making them more visible. Therefore, we performed an experimental study (62) to determine if there were differences in vascular caliber measured on angiographic images obtained with the intravenous injection protocol used for spiral CT versus that used for pulmonary angiography. We measured the diameter of central, segmental, and subsegmental pulmonary arteries in

juvenile pigs by using images obtained during injection of contrast material. The results of our study demonstrate that the site and rate of contrast material injection had no significant effect on porcine pulmonary arterial diameters or pressures when injection was performed at end inspiration. We conclude that the superior detection of PE with angiography compared to contrast-enhanced spiral CT is not attributable to differences in distention of the pulmonary vessels.

2.3.2. A bias induced by an imperfect method of reference (paper 4)?

Most clinical studies evaluating the performance of spiral CT to detect PE use the comparison with pulmonary angiography as a method of reference. We know from different studies that angiography of pulmonary arteries is considered the most specific test for pulmonary thromboembolism and is usually the final and definitive step in the diagnostic work-up of this disorder. Theoretically, sensitivity, specificity and interobserver agreement should reach 100% in a perfect method of reference. However, the standard indexes of diagnostic performance (i.e. accuracy, sensitivity, and specificity) cannot be measured for the arteriographic diagnosis of PE in clinical practice. Quinn et al. (47) have demonstrated that conventional selective pulmonary angiography is reliable in the detection of PE in segmental or larger pulmonary arteries. Observer disagreement becomes considerable for embolus limited to subsegmental pulmonary arteries. Two studies have demonstrated that the inter-observer agreement rates for detection of subsegmental PE ranged between only 45 and 66% (28,29). Diffin et al. (28) have shown that approximately one third of subsegmental emboli and one third of patients with isolated subsegmental emboli may be initially misdiagnosed by pulmonary angiography.

The use of angiography as the gold standard assumes that angiography is always correct. Any errors in the gold standard will always be reported as errors of the method that is being compared. In other words, a subsegmental clot missed on pulmonary angiography and clearly seen on CT will be classified as a false positive result for CT. At the opposite, a misinterpretation

of filling defect as a clot on pulmonary angiography and not depicted on CT will be classified as false negative result for CT.

To verify the accuracy of pulmonary angiography in detecting subsegmental PE, we conducted an experimental study where pulmonary angiography was tested against an independent gold standard (methacrylate cast) (63). Spiral CT was compared to pulmonary angiography and methacrylate cast. We demonstrated that there was no difference in diagnostic performance between spiral CT and angiography for the detection of subsegmental-sized pulmonary emboli and we concluded that spiral CT was comparable to angiography for detection of PE.

2.3.3. Combined veno-CT: a technical innovation to increase the performance of thoracic angio spiral CT (papers 5-6)?

Deep venous thrombosis (DVT) and PE are expressions of a single disease process, namely venous thromboembolism (1-12). Detection of asymptomatic DVT is an indirect way of diagnosing PE.

In 1998, Loud et al. (64) described a new technique for imaging the leg, pelvis, and abdominal veins using the venous opacification that follows rapid infusion of contrast medium of CT pulmonary angiography (Fig.5). We performed a prospective study (65) to test the value of dual-detector helical CT in diagnosing DVT in 65 consecutive patients suspected of acute PE. The results of our prospective study show the excellent performance of dual-slice helical CT venography when combined with chest helical CT in demonstrating DVT. Our study revealed three DVTs among 43 patients (5%) without CT-proven pulmonary embolism. These patients had no signs nor symptoms of DVT, and combined CT venography provided sufficient pertinent data to start the patients on anticoagulation therapy. The sensitivity and specificity of dual-slice CT venography in revealing DVT were 93% and 97%, respectively. This technique had 100% accuracy in the femoropopliteal system. One false-negative and one false-positive diagnoses in our series were probably the result of a lack of enhancement in the infrapopliteal veins. These data are similar to those reported by other researchers who studied patients with suspicion of PE and used collimation as thin as 5 mm for chest and 10 mm for lower extremities. Loud et al. (64) used single-slice helical CT in 71

consecutive patients with combined CT venography and pulmonary angiography and showed 100% sensitivity and specificity. Later on, Loud et al. (66) performed CT venography in 650 consecutive patients and compared the results of CT venography after CT pulmonary angiography and found a sensitivity of 97% and a specificity of 100% for femoropopliteal DVT A comparison of the findings of CT venography with color Doppler sonography for detection of DVT in our study with those of the study of Loud et al. (64) suggests that CT reveals approximately the same number of thromboemboli as sonography and that the error rates are similar. Some investigators recently proposed to use elastic stockings on patients' lower extremities to improve opacification of deep veins (67) but we already applied a similar technique with tourniquets placed at the roots of the lower limbs and ankles with successful results (68).

Concerning the radiation dose delivered to the patient, some researchers (69) have measured organ doses in six patients using thermoluminescent dosimeters placed on the patient's skin prior combined CT pulmonary angiography and venography. The authors showed that the addition of combined CT venography to CT pulmonary angiography increases the gonadal effective dose by a factor of 500 in women and by a factor of 2000 in men. Based on their measurements, the authors conclude that the use of combined CT venography should be carefully considered in young patients.

Figure 5

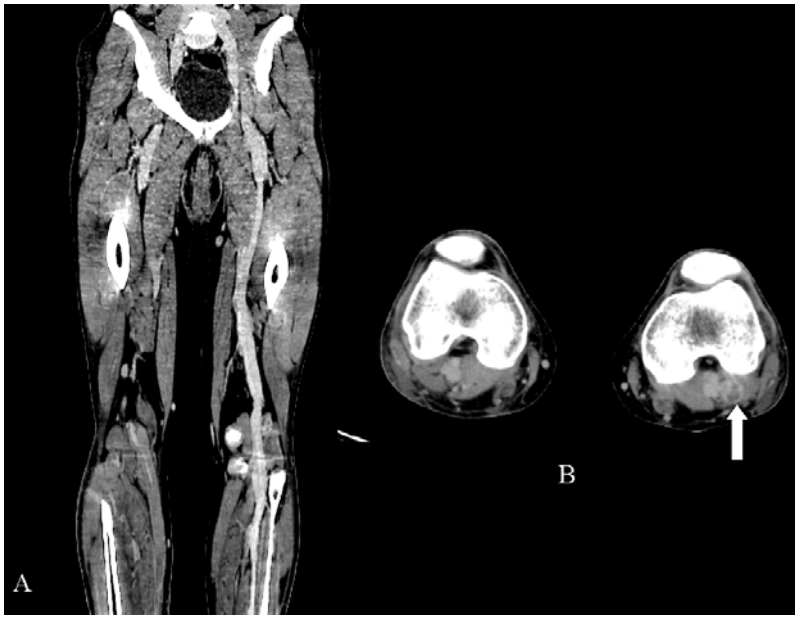

Coronal volume rendered view (A) of a patient with suspicion of acute pulmonary embolism and left lower limb erysipelas. Ultrasound of lower limbs was not performed due to the dermatological problems. A thoracic CT followed by spiral CT of the lower limbs was done on a 16-slice CT unit. Chest CT did not reveal any acute PE. Axial CT views of the lower extremities demonstrate a large necrotic lymph node (arrow) in the left popliteal fossa without any obvious DVT.

3. MULTISLICE CT: A TECHNICAL REVOLUTION

Multislice CT is the latest breakthrough in CT technology. Unlike single-slice CT, multislice can acquire two or more slices in a single rotation (Fig. 6). This faster scanning speed enables the obtention of more and thinner slices. It also reduces or eliminates artifacts produced by patient movement and reduces X-ray tube heating that can constrain single-slice scanning parameters. Today's multislice CT scanners acquire 2, 4, 8 or 16 simultaneous sections. Recently, CT companies have introduced new generations of multislice CT scanners with 32, 40 and 64 rows of detectors. Except for dual slice CT, all multislice CT have more than four rows of detectors in order to accomplish more than one collimation setting. This is achieved by collimating and adding the signals of neighboring detector rows. There are two types of detector arrays: matrix and adaptive arrays. Matrix detectors consist of parallel rows of equal thickness. Adaptive arrays detectors consist of detector rows with varying thickness (70) (Fig.7).

In our institution we have 3 types of multislice CTs: 2 slices, 4 slices and 16 slices systems from *Philips Medical Systems* (Cleveland, Ohio). The *Philips* adaptive array detectors for their four-slice systems consist of eight detector rows of a width that increases from 1 mm for the innermost detector to 1.5, 2.5, and 5 mm for more peripheral detector rows. The latest CT (MX 8000 IDT) installed at the end of March 2002 acquires 16 slices per rotation and the X-ray tube rotation time can go down to 0.42 sec, giving rise to a "Slice Acquisition Rate" which can be as high as 38 slices/second. The Mx8000 IDT detection system consists of a 2D mosaic of solid state detector elements, which, in the longitudinal direction (Z-axis), is divided into 24 rows in an asymmetric configuration: 16 central rows of 0.75 mm each and 8 peripheral rows of 1.5 mm each, for a total detection size of 24 mm (4 x 1.5 mm + 16 x 0.75 mm + 4 x 1.5 mm).

Figure 6

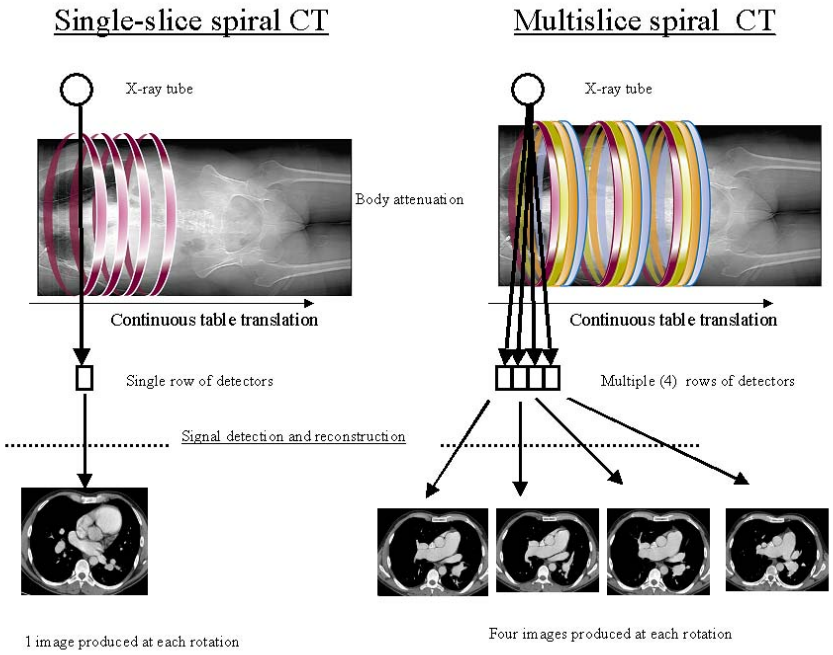

Larger volume coverage and improved transverse resolution can be achieved by simultaneous acquisition of more than one slice and by a shorter gantry rotation time with multislice CT. Technical principles of image acquisition is shown for single-slice and 4-slice CT.

Figure 7

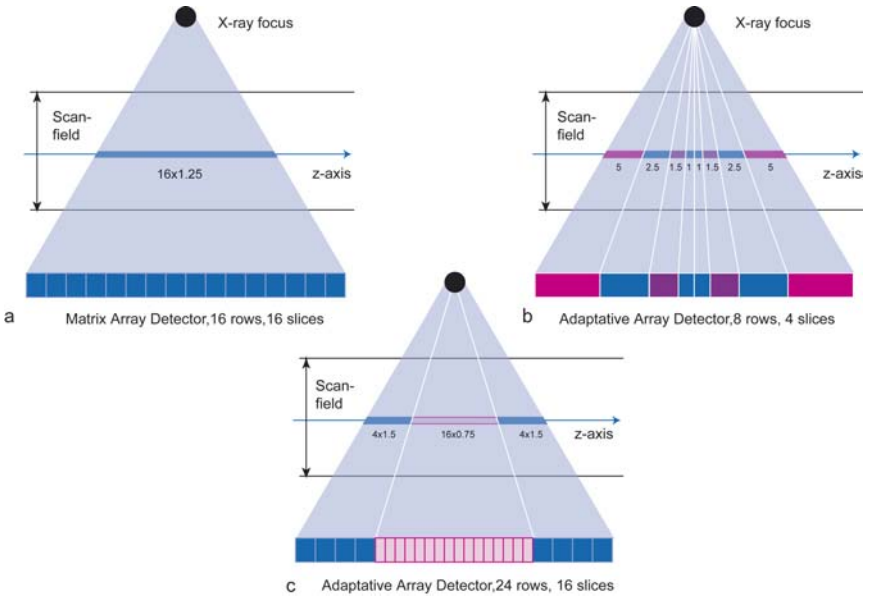

Examples of fixed-array (a) detectors and adaptative (b,c) array-detectors used in commercially available 4-slice and 16-slice CT systems.

The use of multislice CT for the detection of PE enables the acquisition of the entire chest in one breath-hold using 4 x 1 mm (pitch 1.25, 25 seconds acquisition time), 16 x 0.75 mm (pitch 0.95,10 seconds acquisition time) or 16 x 1.5 mm collimation (pitch 0.95, 5 seconds). As a result, more than 300-500 images (if overlapping reconstruction is used) are produced, with a nearly isotropic 3 D image data set of the entire pulmonary arterial tree. The large data load means that new ways of viewing, processing, archiving and demonstrating images are necessary, and that more time is needed to analyze the data than with single-slice spiral CT.

Simon et al. (71) have recently introduced a new concept enabling the visualization of the pulmonary arterial circulation and other lung structures called the paddle-wheel CT display. The authors propose to reconstruct the original data set into a new set of planar reconstructions arranged in a paddle-wheel pattern, in which all planes pass through a central horizontal axis between the two lungs and hilum. Chiang et al. have demonstrated (72) in 5 patients with multiple pulmonary emboli that paddle-wheel reformations had a significantly higher percentage of overall detection of PE than coronal reformations obtained with equivalent slab thickness ($p < 0.0001$).

4. MULTISLICE CT: AN IMPORTANT STEP FORWARD IN THE DIAGNOSIS OF PE?

The advent of a new generation of multi-slice spiral CT, which can cover the entire chest in 1-mm slice thickness in one breath-hold, is expected to result in better analysis of peripheral pulmonary arteries in routine clinical practice with a better depiction of sub-segmental and peripheral thromboemboli. Shorter scanning time is also expected to and has been demonstrated to minimize motion artifacts and reduce the number of inconclusive examinations (73).

4.1. Anatomical studies (paper 7)

We conducted a study (74) on twenty consecutive patients who underwent enhanced-spiral multi-slice CT using 1mm collimation. We identified 769/800 (96%) subsegmental arteries on mediastinal window setting and 1092 out of 2019 sub-subsegmental arteries (54%) on mediastinal window setting. We concluded from our study that enhanced-multislice spiral CT with thin collimation could be used for the precise analysis of the subsegmental pulmonary arteries and even for the identification of more distal pulmonary arteries. We obtained similar results as Ghaye et al. (75) who were able to identify 94% of subsegmental and 74% of sub-subsegmental pulmonary arteries using 1.25 mm thick sections on multislice spiral computed tomography (CT) (4 rows of detectors). Patel et al. (76) also recently showed that multislice CT (4 slices) at 1.25-mm collimation significantly improved visualization of segmental and subsegmental arteries and interobserver agreement in detection of PE.

Raptopoulos et al. (77) compared vascular conspicuity and ability to connect pulmonary arteries on pulmonary angiograms obtained with helical multislice computed tomography (CT) with those of pulmonary angiograms obtained with helical single-slice CT in 93 consecutive patients. The authors concluded that use of multislice CT significantly improved pulmonary arterial visualization in the middle and peripheral lung zones.

4.2. Clinical value: results of a prospective clinical study conducted in the UCL Emergency Department (paper 8,9)

Numerous clinical studies have illustrated the diagnostic value of single-slice spiral CT in demonstrating acute PE (31-38). Its diagnostic value at the segmental level is well established. However, the clinical value of multislice CT and its impact on patient management are not well known. Although multislice CT technology is widely disseminated, there are not yet many accuracy studies to date (Table 3) (78-80).

Some radiologists suggest the selective substitution of spiral CT for ventilation-perfusion nuclear medicine imaging as a screening test for the diagnosis of acute PE (81). Proponents of spiral CT argue that it is more accurate than the usual practice of combining the V/Q scan results and the physician's best clinical judgment. V/Q scan examinations classify patients into groups according to the probability of having pulmonary emboli, whereas the actual thrombus is visible with spiral CT.

Therefore, we conducted a prospective study in our emergency department in 94 patients with suspicion of acute PE (79). All patients had a 4-slice CT (MX 8000, Philips, Cleveland, OH), as well as a V/Q scan within 24 hours. Patients only underwent pulmonary angiography in case of indeterminate or discordant examinations. In our study, thin-collimation multislice spiral CT had a sensitivity of 96% (27/28) and a specificity of 98 % (65/66) for the detection of acute PE. Our results indicated that thin-collimation multislice CT was an accurate method for both the confirmation and the exclusion of PE in outpatients. The rate of inconclusive spiral CT examinations was very low in our series (1%: 1/94) and was significantly lower than V/Q scan examinations ($p<0.005$). The diagnostic accuracy of thin-collimation multislice spiral CT was greater than that of V/Q scan which had a sensitivity of 86% (24/28) and a specificity of 88% (58/66). V/Q scan examinations of intermediate probability were found in 7% of patients (7/94).

In 19 of 66 patients (29%) who did not have PE, thin-collimation multislice spiral CT added diagnostic information that was either suggestive of an alternative diagnosis or was consistent with the final clinical diagnosis. This

additional diagnostic information was neither provided by V/Q scan nor by pulmonary angiography. This represents a serious advantage for spiral CT in these patients (82-83). As reported by Schoepf et al. (84), the use of thin-collimation multislice spiral CT would increase both the sensitivity and specificity in the diagnosis of pulmonary lesions and detection of subsegmental PE (85). Our unpublished data (86) concerning the review of the CT scans obtained from 459 consecutive patients addressed for suspicion of acute PE in our department showed that 4-slice CT revealed PE in 27% of patients. Among those patients with acute PE, 15% had PE that was limited to only subsegmental or more peripheral pulmonary arteries. Forty three percent of those patients with isolated subsegmental PE had pulmonary infarcts demonstrated by CT.

We concluded from this study that thin-collimation multislice CT was a powerful imaging technique for the detection of PE down to the subsegmental level in the evaluation of outpatients. Compared to V/Q scan, multislice CT had a greater diagnostic accuracy with significantly higher rates of conclusive results.

Table 3: Accuracy of spiral CT in the diagnosis of acute PE

	Multislice CT Protocols						
Study	Year	N	Collimation	Lower anatomical level of interpretation	Sensitivity (%)	Specificity (%)	κ Value
Qanadli et al. (78)	2000	157	2 x 2.7 mm	Subsegmental	90	94	0.86
Coche et al. (79)	2003	94	4 x 1 mm	Subsegmental	96	98	0.94
Winner-Muram et al. (80)	2004	93	4 x 2.5 mm	Subsegmental	100	89	0.71

4.3. Diagnostic strategy

Based on our previous clinical work (79), we can provide only some recommendations to physicians for the management of acute PE in an emergency department (Fig.8). However, the diagnostic work-up of PE remains highly dependent on institutional resources and expertise of local radiologists. Emergency physicians and radiologists have to keep in mind that mutlislice CT delivers radiation and necessitates the injection of iodinated contrast agent, which can cause severe allergic reactions and acute renal failure on rare occasions. In our series, although we did not encounter any serious complication related to contrast medium injection, we had to exclude 5% of those patients initially referred for multislice CT with a suspected diagnosis of acute PE because they presented contra-indications for spiral CT, while no patient was excluded from V/Q scan examination in nuclear medicine. Multislice CT is readily available during night and week-ends and its interpretation may be performed by on-call radiology fellows. The overall agreement for interpretations of CT angiograms performed with a 4-slice CT between fellows and attending radiologists was 93% (κ:0.80) in the study performed by Ginsberg and coworkers (87). Discordance often occurred in cases that had technical limitations or concomitant abnormalities.

Therefore we recommend the use of multislice CT in outpatients after exclusion of DVT with Color Doppler ultrasonography and after careful selection of patients including the estimate of the clinical pretest probability of actually having a PE (20-22,88,89) and D-dimer assay levels to save time, cost, and radiation. D-dimers, specific degradation products of cross-linked fibrin, are markers for activation of plasma coagulation and/or fibrinolysis (90). As a general rule, the specificity of D-dimers is too low to confirm PE. In case of raised D-dimer assays (> 500 ng/mL in our laboratory), the physician has to exclude obvious DVT (by lower leg Doppler ultrasonography) and other alternative obvious differential diagnoses that could have raised D-dimers, such as an infection or inflammatory process. A negative D-dimers assay has been shown to have a strong negative predictive value for acute venous thromboembolism (91-94).

A number of studies have shown that the risk of PE after an initial negative CT angiography is about 1% (73).

Multislice CT is particularly useful in patients who have conditions that result in non diagnostic V/Q scan examinations, such as those with significant cardiopulmonary disease, chronic obstructive pulmonary disease or infiltrates on chest radiography. Indications of multislice CT will be intensively discussed with physicians referring young patients and avoided in patients with poor renal function or allergy to iodine.

The combination of chest CT with venography (64-66) is interesting in patients with assessment difficulties by ultrasonography, such as patients with a leg cast, edema of lower limbs, or limited mobility, or those in centers where trained radiologists are not available for performing ultrasound examination.

Figure 8: Diagnostic strategy for suspicion of acute PE

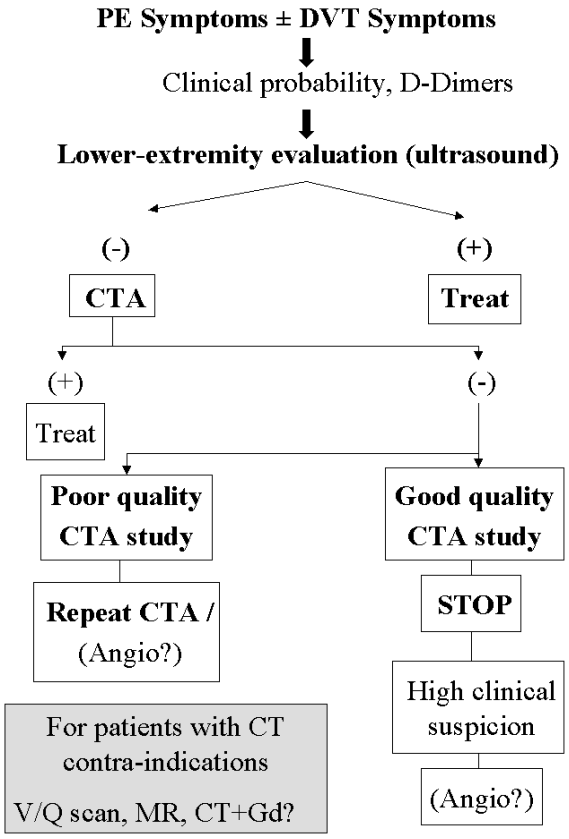

Modified from reference 95

5. DOSE CONSIDERATIONS

Radiation exposure during diagnostic work-up of pulmonary embolism (paper 10):

An important question that remains to be addressed before routinely performing multislice CT for PE work-up is the radiation dose delivered during this procedure compared to the current gold standard of pulmonary angiography. Resten et al. (96) have recently compared the radiation doses delivered by single-slice CT and pulmonary angiography (PA). Average doses were approximately five times smaller with spiral CT than with pulmonary angiography (6.4+/-1.5 mGy and 28+/-7.6 mGy, respectively). The most important doses were abreast the pulmonary apex for CT, and abreast the pulmonary arteries for PA. Compared with pulmonary angiography, spiral CT dose distribution was relatively uniform (10-13 mGy). Kuiper et al. (97) have recently compared the effective dose of 4-slice CT and digital subtraction angiography during pulmonary embolism work-up. They obtained an average effective dose for multislice CT angiography of the pulmonary arteries of 4.2 mSv (range 2.2-6.0 mSv) and an average effective dose of 7.1 mSv (range 3.3-17.3 mSv) for digital subtraction angiography.

In collaboration with radiation physicists, we have simulated CT protocols (4 x 1 mm or 16 x 0.75 mm, 120 Kv, 144 mAs, pitch: 1.25) with 4-slices (MX 8000 Quad) and 16-slices (MX 8000 IDT) CT using an anthropomorphic phantom (Alderson Phantom), and compared them to the radiation dose delivered during pulmonary angiography using the same method (paper submitted). The mean radiation dose delivered at the level of the middle part of the chest was 21.5 mGy, 19.5 mGy and 18.2 mGy for 4-slice CT, 16-slice CT without and with dose modulation program (Dose right, Philips Medical system, The Netherlands) respectively. Dose modulation program is a dedicated software available for MX 8000 IDT (version 2.5 software) and modulates the tube current according to the patient body attenuation. This system was available only for the last generation of multislice CT at the time of experimentation. This system uses each rotation to determine the next rotation modulation and reduces the mA in the direction

of the high signal (98-100). This software should save dose in rotationally asymmetrical objects without compromising image quality (101).

From our experimentation we were able to draw three main conclusions, which we believe are important: 1/ Higher radiation doses are delivered by digital pulmonary angiography than by multislice CT. We found different radiation doses than Resten et al. (96) but experimental conditions were not the same as ours and the results are difficult to compare. Variations in patient doses are large for pulmonary angiography because the number of incidences and time of fluoroscopy vary according to the expertise of the radiologist, the medical state of the patient and the difficulty of the clinical case. For CT technology, the protocol is more standardized and in the vast majority of patients, the radiologist carries out only one acquisition of the pulmonary arteries. 2/ Dose distribution is less homogeneous on pulmonary angiography than on multislice CT and is a function of complexity of examination. The ratio of the maximum dose to the mean dose was 1.15 and 3 for CT and angiography respectively. The heterogeneity on pulmonary angiography is related to the important attenuation of the X-rays (102,103) with depth and to the fact that the total dose results from four incidences not homogenously distributed within the anatomic volume. 3/ The delivered radiation doses decrease with the use of multislice CT with the highest multislice factor and online tube current modulation program. Physics shows that the dose delivered by a CT scanner is influenced by many factors and parameters (102). Among those factors, some are “intrinsic” and inherent to the design of the CT scanner so that they cannot be modified by the CT user as for example: the X-ray tube and its filtration, the geometry of the CT scanner, the collimator settings. Those parameters were identical on both CT units used in this study as well as the trapezoidal collimated dose profile (103,104). With multislice CT, only the plateau region of the dose profile may be used to ensure equal signal level for all detector slices. The penumbra region has to be discarded, either by a post-patient collimator, or by the intrinsic self collimation of the multislice CT, and represents “wasted dose” (Fig.9). The relative contribution of the penumbra region decreases with increasing number of simultaneously acquired slices and increases with

decreasing slice width (103,104). This physical property explains the relative lower dose we obtained with 16-slice CT compared to 4-slice CT (Fig.10).

We recently verified this physical property by measuring CTDI on 3 multislice CT available in our department (105) (Dual CT, MX 8000 Quad and MX 8000 IDT) with the same geometry, tube filtration and acquisition parameters. For thin slices (120 kV, 100 mAs) the $CTDI_w$ obtained was 18.55 mGy (Dual: 2 x 1 mm), 15.70 mGy (Quad: 120 kV, 4 x 1 mm) and 13.75 mGy (IDT:16 x 0.75 mm). Normalized $CTDI_w$ were 31.88, 24.33 and 8.25 mGy respectively. We concluded from this study that, for thin-slice reconstructions, it is recommended to use a CT scanner with the highest multi-slice factor available (≥16).

The use of the modulation dose program on the most recent multislice CT unit can decrease radiation dose especially to the upper part of the chest.

The mean value of radiation exposure was decreased by 10-15% at the level of the upper chest and by about 5% at the level of the middle and lower part of the chest with the dose modulation program. Mastora et al. (101) evaluated image quality obtained with anatomically adapted online tube current modulation and preset minimum dose savings at multi–detector row spiral computed tomographic (CT) angiography of the thoracic outlet in 100 patients. They obtained 35% reduction in mean current-time product, with no loss in image quality. Further studies comparing image quality regarding detection of PE should be realized in the near future. Decrease of tube current with acceptable image quality for diagnosis of PE is possible as suggested by Tack et al. (106).

A survey of practices and policies revealed that members of the Society of Thoracic Imaging perform CT angiography in pregnant women (107). Forty percent respondents reported that they made modifications to reduce radiation exposure for pregnant patients. The most common modification reported was to decrease the scanning area along the z-axis. Other modifications included increasing pitch, reducing field of view, eliminating frontal and lateral scout images, reducing milli-ampere-seconds, reducing peak voltage, and thickening detector collimation. A recent study demonstrated that the average fetal radiation dose received by helical CT was less than by ventilation-perfusion lung scan during all trimesters (108).

Figure 9

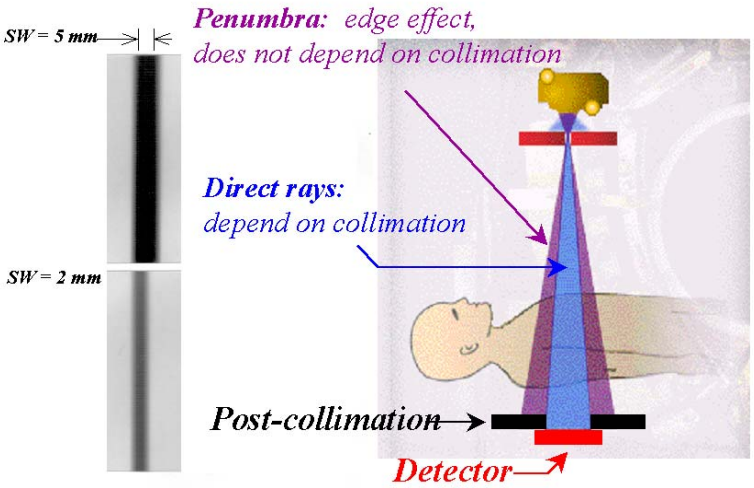

Schematic representation of direct radiation and penumbra effect in CT.

Figure 10

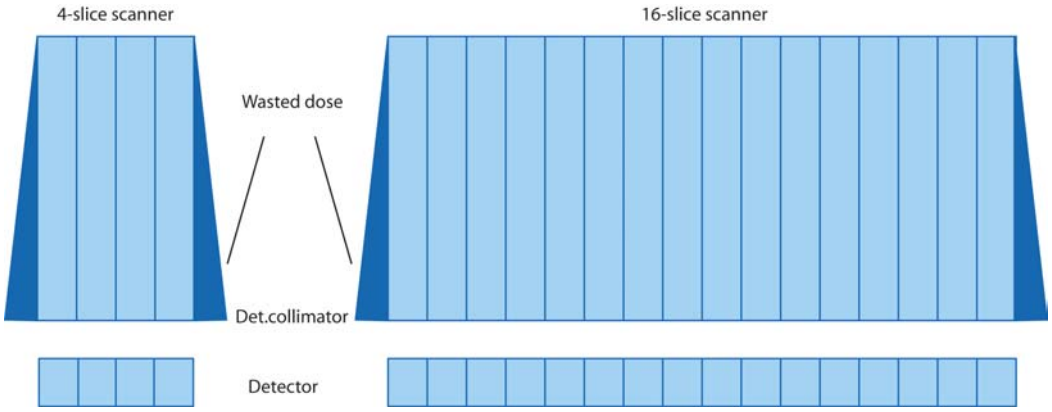

Doses profiles for a 4-slice CT system and a 16-slice CT system with equal collimated width of one detector slice. The relative contribution of the penumbra region, which represents wasted dose, decreases with increasing number of simultaneously acquired slice.

6. PERSPECTIVES

6.1. Optimization of contrast medium injection

There is no consensus concerning the optimal dose and rate of contrast medium to use in order to analyze the pulmonary arteries (54). Yankelevitz et al. reported the total volume, injection rate from each of 10 protocols concerning CT angiography of pulmonary arteries in the literature with single-slice CT. Reported infusion rates in the literature varied between 2 to 5 ml/sec with the total contrast amount varying between 80 to 140 ml. Because of the reduced window of data acquisition with multislice CT and individual factors such as cardiac output, venous access, the optimal contrast medium delivery is becoming increasingly difficult to achieve. The shorter acquisition time associated with multislice CT suggests that either the injection rate should be increased if the contrast medium density is maintained, or a lower volume injected but with higher concentration of contrast medium if injection rates are to be kept constant (109) (Appendix 8.1). Kirchner et al. (110) demonstrated that the use of a real time bolus triggering system with a 4-slice CT was able to reduce contrast material in chest CT examinations. The mean amount of contrast material required to reach a threshold level of 100 HU over the baseline in pulmonary arteries was obtained with 48.2 ±10.7 ml.

The use of a saline chaser coupled with high-speed acquisition should decrease the amount of contrast material, provide substantial cost savings and possibly reduce nephrotoxicity. No data exist in the literature concerning potential reduction of contrast medium in chest CT with this injection system but some authors have conducted similar experiences with abdominal CT (111). The authors were able to decrease the amount of contrast medium by 30% (100 ml versus 150 ml) with no significant difference in liver parenchyma attenuation or lesion conspicuity.

We can imagine new challenges in the near future, as new multislice CT units with 40 or 64 rows of detectors will dramatically decrease CT acquisition time, thereby leading to subsequent difficulties in optimizing contrast medium enhancement. A computer-based, physiological model that may help predict vessel-specific and organ-specific CT contrast medium

enhancement for different injection protocols should be developed (112) by the industry in collaboration with radiology research.

6.2. Use of alternative contrast media (paper 11)

The main limitation of CT angiography of pulmonary arteries is related to the use of iodinated contrast medium, which is contra-indicated in patients with renal failure or iodine allergy. We therefore tested the use of gadolinium, known for its reduced side-effects, in a patient allergic to iodine with suspicion of PE (113). The amount we used in this study was 60 ml of Gadodiamide (0.4 mMol/kg of body weight) and the peak enhancement measured in our patient was 103 ±15 HU in the main pulmonary artery and was adequate to detect endovascular emboli without any adverse effects.

The use of gadolinium in CT was first described by Bloem et al. in 1989 (114). The authors demonstrated that the appearance of the urinary collecting system at Gd-DTPA-enhanced CT imaging was similar to that on iodine-enhanced CT images. The opacification of the urinary tract was interpreted as the result of the high atomic number (64) of gadolinium, which compares favorably with that of iodine (53). Its higher k-edge (50 KeV, compared to 33 KeV for iodine) is better matched to the peak intensity of the post filtration energy spectrum produced during CT scanning which is around 50-60 KeV for studies performed at 80-140 kVp with current CT scanners (115). At the same molar concentration, gadolinium produces a greater attenuation than iodinated contrast medium during CT scan examinations. Quinn et al. (116) showed that Gd-DTPA can be used to provide enhancement during CT imaging and might be of value in iodine-sensitive patients at a dose of 0.5 mMol/kg. Dynamic gadolinium-enhanced CT examinations were performed in another experimental study using three pigs (115). The authors demonstrated that the mean peak of enhancement in pulmonary arteries was 168 HU using a 50 ml bolus of Gadodiamide (0.8-1.0 mMol per kilogram of body weight at a rate of 2 ml/sec).

Recently, Remy-Jardin et al. (117) injected Gd-DTPA on sixteen-slice CT in 54 patients suspected of having acute PE. The authors obtained diagnostic image quality in 94% of gadolinium-enhanced CT angiograms. The dose

administered did not alter renal function except in one case. Bae et al. (118) tested Gadolinium contrast medium in pigs combined with multislice computed tomography and concluded that gadolinium may provide clinically useful CT angiography examinations.

6.3. Automatic recognition of PE

CT examination for the detection of PE currently requires radiological analysis of 400 to 600 images. The computer-aid can be used as a screening tool to detect vascular defects related to PE. Recently, a computer-assisted diagnostic (CAD) tool was developed for the diagnosis of acute PE in perfusion lung scans (119). Shoepf et al. developed a CAD of segmental and subsegmental pulmonary emboli on 1-mm multislice CT (120). The authors demonstrated in 15 consecutive patients that application of CAD tools may improve the diagnostic accuracy and decrease the interpretation time of CT angiography. Masutani et al. evaluated a fully automated method for computerized detection of PE in spiral CT (121). Preliminary results suggest that the method has potential for fully automated detection of pulmonary embolism. We are currently developing automatic segmentation of pulmonary arteries and automatic detection of pulmonary embolism in collaboration with the Universities of Mons and Louvain-La-Neuve. Clinical applications should be tested in the near future (appendix 8.2)

6.4. Functional imaging

6.4.1. Perfusion evaluation

With the advent of fast CT scanning techniques, functional parameters of lung perfusion can also be assessed non-invasively by multislice CT. In recent years, electron-beam CT has been used both for volume scanning to reveal intravascular thromboemboli and for pulmonary blood flow measurements (122). The speed of the electron-beam CT scanner enables imaging of the thoracic vessels during optimal contrast opacification. Perfusion defects on CT allow the direct parenchymal assessment of the extent of PE, especially for isolated subsegmental emboli. This information is reliably given by pulmonary angiography and V/Q scan. In order to facilitate visualization of

parenchymal enhancement, color encoding and subtraction software are usually used.

6.4.2. Pulmonary embolism severity and cardiac assessment (paper 12)

Previous papers have shown that severity of acute PE could be evaluated by quantitative CT scores mainly based on the overall amount of clot burden within the pulmonary vasculature. The degree of pulmonary artery obstruction is well correlated with clinical severity of PE (123-126) and may be relevant for patient treatment (127) and prognosis.

Moderate to massive PE may be associated with right ventricular dysfunction. Among patients with PE, those with right ventricular dysfunction have a worse prognosis and are at increased risk of recurrent PE and death than those with a normal right ventricular function (128,129). Spiral CT might play a role in detecting right ventricular dysfunction on static cross-sectional images (130,131). A single exploration that accurately defines pulmonary arteries, lungs and global cardiac function on dynamic images would be desirable because the function of the right heart after PE is a major prognostic factor.

Indeed, a method for cardio-thoracic multislice spiral CT imaging with ECG gating for suppression of heart pulsation artifacts has recently been introduced (132). The proposed technique offers extended volume coverage compared with standard ECG-gated spiral CT scan. By using this approach cardiac pulsation and artifacts in paracardiac lung segments can be effectively reduced and detection of PE should be improved in the above-mentioned areas. Dynamic evaluation of the cardiac tissues, the valves and any emboli can be performed using data obtained throughout different periods of the heart cycle. Since measurement of left ventricular ejection fraction has been accurately calculated by retrospective analysis of ECG-gated multislice spiral CT (MSCT) data sets (133), we can suppose that right ventricular function could also accurately be determined using the same technique during PE work-up. This technique is currently evaluated with a 16-slice CT in our department of medical imaging (134). Ten patients with a suspected diagnosis of PE were assessed by ECG-gated CT and planar radionuclide ventriculography within 24 hours. Right and left ventricular ejection fractions

were measured with both methods. A good correlation was obtained for right (R = 0.89) and left ventricular (R = 0.91) ejection fractions with better results for the left ventricle than for the right ventricle. The main limitations were related to tachycardia and severe dyspnea (Appendix 8.3). Inter and intra-observer variability for measuring right ventricular function was recently evaluated in a series of 18 patients addressed for suspicion of acute PE (135). The intraclass correlation for two observers for measuring right ventricular end-diastolic volumes, end-systolic volumes and ejection fraction was 0.97. The intraclass correlation for one observer for measuring the same parameters was 0.98, 0.98 and 0.94 respectively.

Another potential application of whole chest CT acquisition with ECG gating resides in a full comprehensive chest examination for the patient with chest pain (Appendix 8.4). Using this technique, an entire chest can be covered in a single breath-hold of roughly 20 seconds with a good spatial resolution. Recently we have assessed two patients addressed for atypical chest pain and we were able to detect acute myocardial infarction and exclude other causes of chest pain including PE, aortic dissection, and pulmonary disease, from one scan with one single shot of contrast.

6.5. Integration with other imaging modalities (paper 13)

Chest radiograph is usually the first-line imaging modality performed in patients with suspicion of acute PE. It is well recognized that interpretation of chest X-ray is difficult and often interpreted by junior residents in radiology. In fact, both senior and junior radiologists of our UCL Imaging Department currently have the opportunity to correlate the different abnormalities seen on chest radiographs with images obtained with multislice CT (136). The use of multislice CT with isotropic acquisition results in increased image quality with different views that can be reformatted in any desired plane. Picture Archiving Communication Systems (P.A.C.S.) and special flat panels for thoracic radiography will be installed in our department in the near future, thereby providing radiologists with invaluable opportunities to perform such side-by-side correlations with chest CT, chest MR or V/Q scan examinations.

6.6. Technical developments

The evolution of CT technology will happen through the adjunct of additional rows of detectors and a decrease in rotation time. New multislice CT units with 40, 64 rows of detectors and a rotation time $\leq$ 0.4 seconds are already currently emerging on the radiological market (appendix 8.5). Our preliminary results performed in association with the University of Utrecht concerning the delivered radiation dose of the new 40-slice CT (MX 40Brillance) are encouraging and demonstrate a reduction in radiation dose. New detectors such as flat panels are under consideration for future developments of CT scanners (137-139).

This technical progress will directly benefit detection of PE by overcoming current technical limitations and pave the way for continuing increased accuracy in diagnosis.

7. CONCLUSIONS

During the course of this thesis, we have demonstrated the following points

1/ Pulmonary arterial distension is not significantly reduced during spiral CT, and the failure of single-slice CT to detect subsegmental PE is not attributable to this fact.

2/ Single-slice spiral CT has the same diagnostic accuracy as pulmonary angiography to detect sub-segmental PE but its diagnostic performance in clinical studies is hampered by systematic comparison with an imperfect method of reference (pulmonary angiography).

3/ Combined veno-CT could demonstrate the source of emboli and, in some patients, lead to the initiation of anticoagulant therapy when no evidence of acute PE could be found on spiral chest CT examination.

4/ The advent of multislice CT enabled a better identification of peripheral pulmonary arteries.

5/ The use of thin-collimation multislice CT in out-patients enabled accurate diagnosis of PE down to the subsegmental level and revealed alternative diagnoses in patients without PE on high-quality isotropic examinations.

6/ Multislice CT delivered less radiation dose than pulmonary angiography. Application of dose modulation programs further decreases the delivered radiation dose.

7/ Recent developments of CT technology should lead to a reduction in radiation dose and in the amount of contrast medium delivered to the patient. More sophisticated techniques such as ECG-gated acquisition and perfusion imaging should give some additional functional and morphological information

affecting prognosis, repercussions and differential diagnosis of the thromboembolic event.

We can conclude at this stage of knowledge that multislice CT is an accurate technique to detect acute PE. This technique may provide alternative diagnoses and demonstrate the source of emboli during the same examination time. This technique is continuously evolving and can currently already provide some functional parametric data in addition to morphological data that are highly likely to influence the treatment and prognosis of thromboembolic disease.

8. APPENDIX: SOME RECENT DEVELOPMENTS

8.1. Diagnosis of pulmonary embolism with 16-slice CT scanners

A 42-year-old male patient was referred to our radiology department for progressive dyspnea and chest pain over the last few days. The patient was known to have lung cancer with widespread metastases. On clinical examination, the patient presented a moderately raised temperature of 38°C and a tachycardia (118 beats/min) with a paradoxical pulse; his blood pressure measurement was 115/80 mmHg. Cardiac auscultation revealed reduced heart sounds. There was no evidence of thrombophlebitis of the lower limbs. A chest radiograph revealed a moderately enlarged heart size with bilateral pleural effusions. A CT pulmonary angiography of the chest was performed using multislice spiral CT (Philips MX 8000 IDT, The Netherlands) which is able to acquire 16 slices of 1 mm per sub-second rotation time. Scanning parameters were the following: 16 x 0.75 mm collimation, 0.42 sec tube rotation time, 1mm reconstructed slice thickness with 50% overlap, pitch of 1.2. Seventy milliliters of iodinated non-ionic contrast agent (Xenetix, Guerbet, France), were injected at 3 ml/sec rate and image acquisition started after 18 seconds. The acquisition time was 10 seconds and 340 axial images were generated. Images were analyzed on a cine mode on a workstation (MX view, Philips, The Netherlands) using mediastinal window setting (WL 50 HU, WW 350HU), lung window setting (WL: 50 HU, WW: 350 HU), multiplanar reformations and 3D volume rendering reconstructions.

A large pericardial effusion containing several soft tissue masses, consistent with a carcinomatous pericarditis was observed on multislice CT examination (curved arrows). Hypodense clots (straight arrows) were visualized in segmental arteries of the right middle lobe and its peripheral branches on axial CT, oblique reformatted images (Fig. 1) and 3D volume rendering reconstructions (Fig. 2). A peripheral triangular pleural-based consolidation (Humpton's hump) consistent with pulmonary infarction was seen in the external segment of the right middle lobe (broad arrow).

This case highlights the ability of the new generation of CT scans to acquire images of the whole lungs in millimetric axial sections in 10 seconds or less.

The resulting shorter acquisition time allows ***to reduce drastically the amount of iodinated contrast agent (70ml or less)*** used in the diagnosis of thromboembolic diseases. The near-isotropic resolution of this new type of CT provides high quality images with superior multiplanar and 3D image reconstructions of the pulmonary circulation.

Figure 1

Figure 2

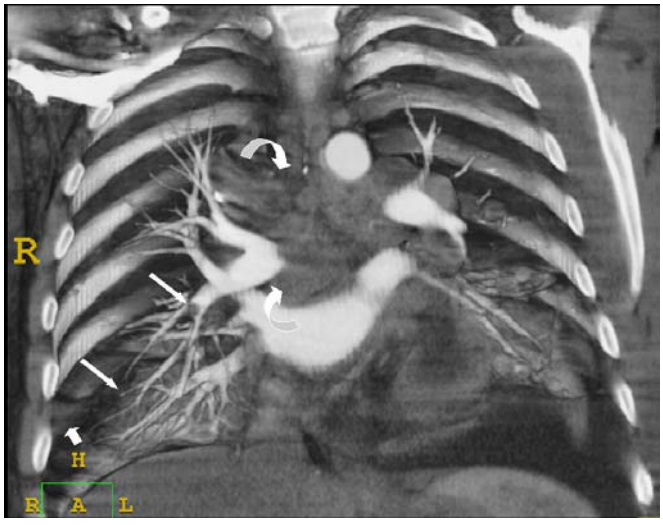

From reference 140

8.2. Automatic segmentation of pulmonary arteries and detection of acute pulmonary embolism

Figure 1

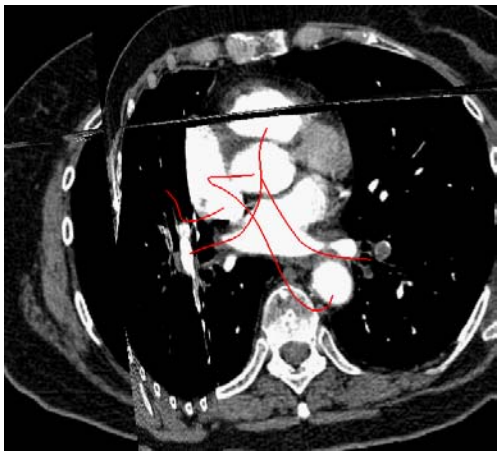

Automatic detection of PE is a challenging task. First, researchers have to delineate automatically pulmonary arteries by segmentation. Many methods have been presented for handling segmentation of elongated shapes. Region growing methods have shown a superior ability for the segmentation process. However, close contacts between pulmonary arteries and systemic vessels represent a real problem because the front propagation method does not recognize the proper boundaries. For this reason, we decided to combine the a priori anatomical knowledge of the course of the vessels to recreate the missing boundaries and guiding the segmentation process. In this experiment, pulmonary arteries, aorta and superior vena cava have been modelled as 3D curves in order to separate automatically these structures intensely filled with contrast medium from each other.

Figure 2

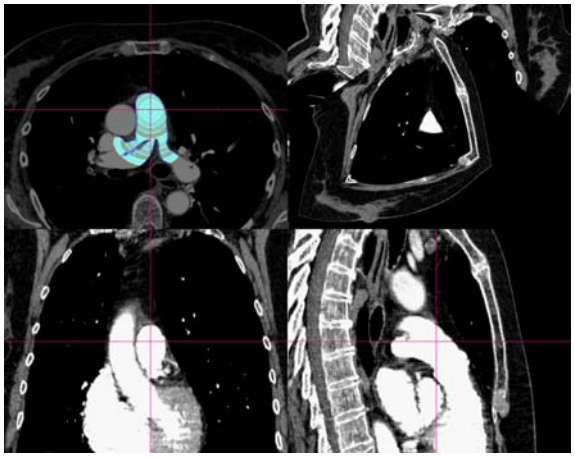

Result of the segmentation process: pulmonary arteries boundaries appear in blue, slice boundaries in gray. The pulmonary embolus appears as a dark spot surrounded by color.

Courtesy of Raphaël Sebbe, Faculté polytechnique, University of Mons

8.3. Acute pulmonary embolism with ECG-gated 16-slice CT and evaluation of potential right heart repercussion

A 81-year-old woman with high clinical suspicion of acute PE.

Images obtained at the end-diastolic (Fig.1) and end-systolic (Fig.2) phases of the cardiac cycle, from multislice CT and reformatted in an oblique plane demonstrated a large pulmonary embolism located in the left pulmonary artery (arrow). Right ejection fraction was measured at 43% and 41% on multislice CT and radionuclide ventriculography respectively. Left ejection fractions were evaluated at 68% and 65% respectively by the same techniques. Note the variation of the right ventricular volumes throughout the cardiac cycle (curved arrows) on the static images.

Figure 1 **Oblique reformatted CT Image obtained at end-diastolic phase**

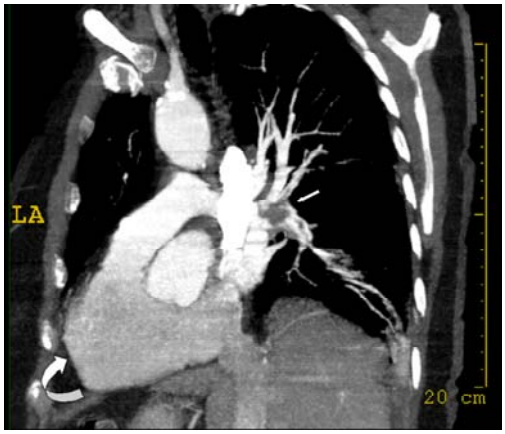

Figure 2 **Oblique reformatted CT Image obtained at end-systolic phase**

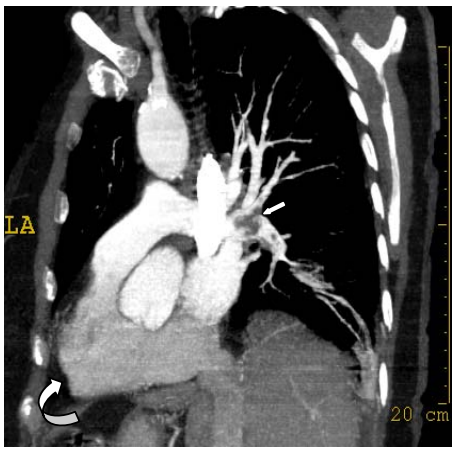

8.4. Assessment of atypical acute chest pain in emergency room with ECG gated 16-slice CT of the whole chest: Pulmonary embolism or myocardial infarction?

A 76-year-old man presented to our emergency department reporting one night of persistent mild constrictive thoracic pain irradiating between both scapulae. His past medical history was notable for arterial hypertension, hypercholesterolemia and left iliac artery occlusion. The patient's initial vital signs included a heart rate of 61 beats/min, blood pressure readings of 135/75 mmHg in the right arm and 144/76 mmHg in the left arm. A first ECG did not show any acute ischemic pattern. Blood sample revealed a troponin value of 1.15 ng/ml (normal troponin values: < 0.06 ng/ml). A CT scanner of the chest was requested in order to rule out an acute aortic dissection or pulmonary embolism.

Retrospective ECG-gated 16-slice CT (Philips Medical Systems, Cleveland, OH) of the entire chest was performed in one breath-hold after injection of contrast medium with 16 x 1.5 mm collimation. No aortic dissection and no pulmonary embolism were seen but reformatted oblique images (panel 1A) reconstructed during the diastolic phase revealed severe stenosis of the left subclavian artery (curved arrow), an irregular right coronary artery (RCA) with an acute occlusion of its distal portion (straight arrow). Frontal view performed at the middle part of the left ventricle (panel 1B) demonstrated a hypoperfused area of the myocardium at the inferior part of the left ventricle (straight arrows). Curved image reconstruction (panel 1C) performed in the plane of the RCA delineates more precisely the site of the RCA occlusion (straight arrow). The patent right coronary artery appears in red and the occluded vessel appears in green on the color-graded image (panel 1D). Angiography of coronary arteries (panel 1E) confirmed the CT findings with an occlusion of the distal portion of the RCA (straight arrow).

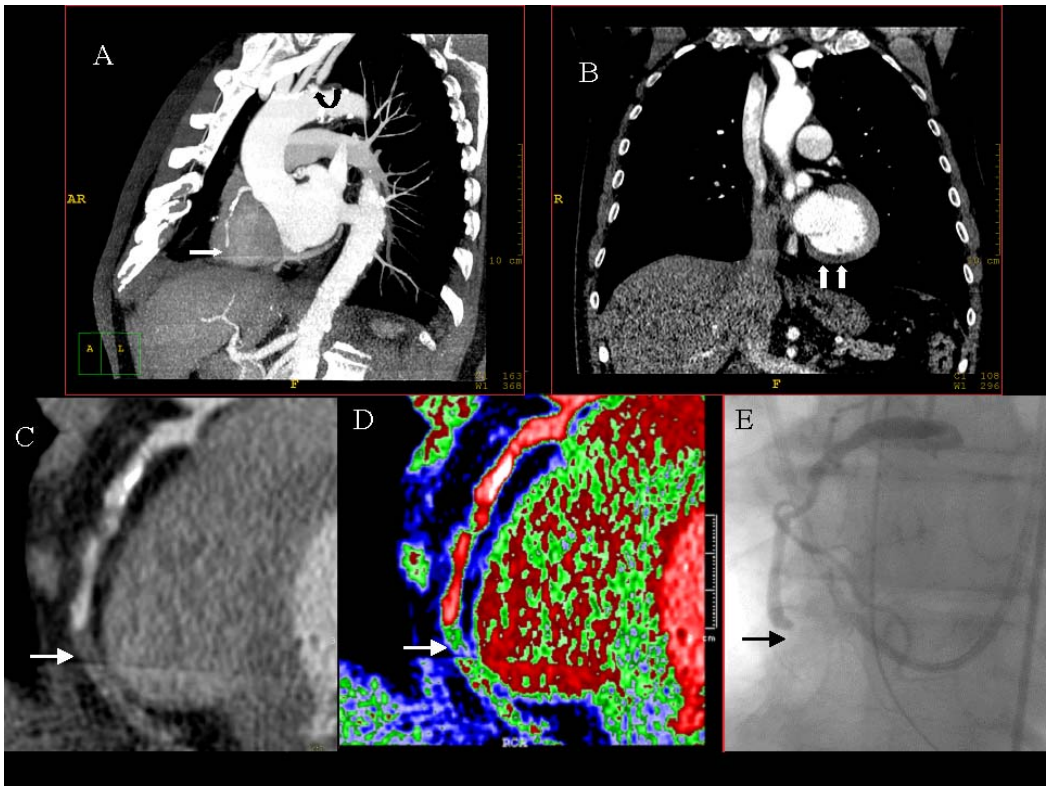

From reference 141

In conclusion, current medical imaging developments may help the clinician facing a difficult differential diagnosis of thoracic pain by showing acute ischemic lesions in the coronary tree and excluding other causes of thoracic pain such as acute pulmonary embolism or aortic dissection.

8.5. Tricuspid valve endocarditis and acute pulmonary embolism with ECG-gated 40-slice CT of the whole chest

A 41-year-old male drug addict was referred to our institution for fever and respiratory failure. Bedside chest X-ray revealed multiple lung nodules disseminated throughout both lungs. Blood culture revealed Staphylococcus aureus.

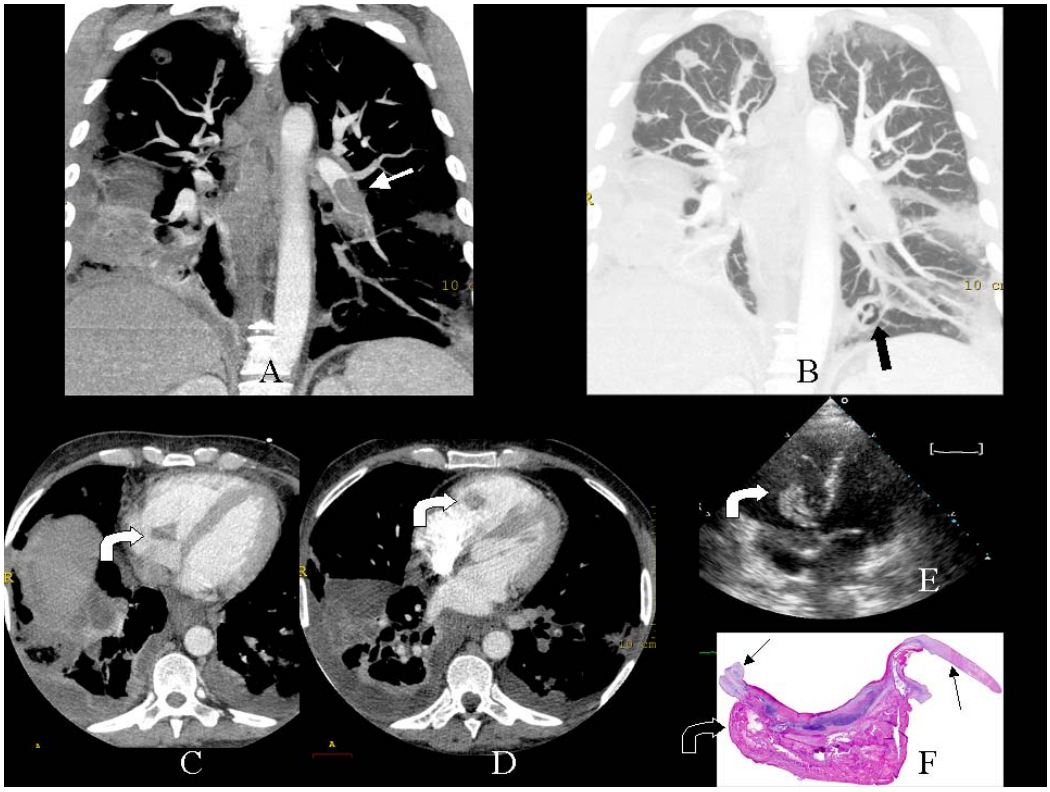

Retrospective ECG-gated 40-slice CT (MX Brilliance 40, Philips Medical Systems, Cleveland, OH) of the entire chest was performed with 40 x 0.625 mm collimation, 1 mm interval reconstruction, 120 Kv and 400 mAs/slice. The entire chest was imaged in one breath-hold during 20 seconds, after injection of 120 ml of contrast medium. Heart rate was 110 beats/min during CT acquisition.
Frontal reformatted images of the entire chest demonstrated on Maximal Intensity Projection (MIP) (Panel A) and mediastinal window setting a large filling defect occupying the left inferior pulmonary artery (straight arrow). Multiple nodules of various sizes, some excavated (straight arrow) and suggestive of septic emboli were well depicted on lung window setting (Panel B).
During the same examination, CT images were reconstructed retrospectively at diastolic (Panel C) and systolic phase (Panel D) and revealed a rounded hypodense masse (curved arrow) implanted on the tricuspid valve.
Transesophageal echocardiography (panel E) revealed a mobile vegetation (straight arrow) implanted on the tricuspid valve (curved arrows).
The patient was operated and pathological specimen (panel F) showed a large vegetation attached to the tricuspid valve (straight arrows)

In the present case, ECG-gated multislice CT of the chest led to a combined diagnosis of acute pulmonary embolism, tricuspid valve endocarditis and septic pulmonary embolism on the same imaging modality. Acute PE was probably due to the migration of septic material from the tricuspid valve into the pulmonary arterial circulation (142).

9. REFERENCES

9.1. General References

1. Kruit WH, de Boer AC, Sing AK, Van Roon F. The significance of venography in the management of patients with clinically suspected pulmonary embolism. J Intern Med 1991; 230(4): 333-339.
2. Hull RD, Hirsh J, Carter CJ, Jay RM, Dodd PE, Ockelford PA, Coates G, Gill GJ, Turpie AG, Doyle DJ, Buller HR, Raskob GE. Pulmonary angiography, ventilation lung scanning and venography for clinically suspected pulmonary embolism with abnormal perfusion lung scan. Ann Intern Med 1983; 98(6): 891-899.
3. Turkstra F, Kuijer PM, van Beek EJ, Brandjes DP, ten Cate JW, Buller HR. Diagnostic utility of ultrasonography of leg veins in patients suspected of having pulmonary embolism. Ann Intern Med 1997; 126(10): 775-781.
4. Quinn RJ, Nour R, Butler SP, et al. Pulmonary embolism in patients with intermediate probability lung scans: diagnosis with Doppler venous US and D-dimer measurement. Radiology 1994; 190(2): 509-511.
5. Girard P, Musset D, Parent F, Maitre S, Philippoteau C, Simonneau G. High prevalence of detectable thrombosis in patients with acute pulmonary embolism. Chest 1999; 116(4): 903-908.
6. Dorfman GS, Cronan JJ, Tupper TB, Messersmith RN, Denny DF, Lee CH. Occult pulmonary embolism: a common occurrence in deep venous thrombosis. Am J Roentgenol 1987; 148(2): 263-266.
7. Huisiman MV, Büller HR, ten Cate JW, et al. Unexpected high prevalence of silent pulmonary embolism in patients with deep venous thrombosis. Chest 1989; 95(3): 498-502.
8. Nielsen HK, Husted SE, Krusell LR, Fasting H, Charles P? Hansen HH. Silent pulmonary embolism in patients with deep venous thrombosis. Incidence and fate in a randomized, controlled trial of anticoagulation versus no anticoagulation. J Intern Med 1994; 235(5): 457-461.
9. Moser KM, Fedullo PF, LittleJohn JK, Crawford R. Frequent asymptomatic pulmonary embolism in patients with deep venous thrombosis. JAMA 1994; 271(3): 223-225.
10. Prandoni P, Polistena P, Bernardi E, et al. Upper-extremity deep vein thrombosis. Risk factors, diagnosis, and complications. Arch Intern Med 1997; 157(1): 57-62.
11. Monreal M, Raventos A, Lerma R, et al. Pulmonary embolism in patients with upper extremity deep venous thrombosis associated to central venous lines: a prospective study. Thomb Haemost 1994; 72(4): 548-550.
12. Monreal M, Lafoz E, Ruiz J, Valls R, Alastrue A. Upper extremity deep venous thrombosis and pulmonary embolism: a prospective study. Chest 1991; 99(2): 280-283.
13. Silverstein MD, Heit JA, Mohr DN, Petterson TM, O'Fallon WM, Melton LJ 3rd. Trends in the incidence of deep vein thrombosis and pulmonary embolism: a 25-year population-based study. Arch Intern Med 1998; 158(6): 585-593.
14. Miniati M, Pistolesi M, Marini C, et al. Value of perfusion lung scan in the

diagnosis of pulmonary embolism: results of the Prospective Investigative Study of Acute Pulmonary Embolism diagnosis (PISA-PED). Am J Respir Crit Care Med 1996; 154(5): 1387-1393.
15. The PIOPED Investigators. Value of the ventilation/perfusion scan in acute pulmonary embolism. Results of the prospective investigation of pulmonary embolism diagnosis (PIOPED). JAMA 1990; 263 (20): 2753-2759.
16. Hull RD, Hirsh J, Carter CJ, et al. Diagnostic value of ventilation-perfusion lung scanning in patients with suspected pulmonary embolism. Chest 1985(6); 88: 819-828.
17. Goldhaber SZ, Visani L, De Rosa M. Acute pulmonary embolism: clinical outcomes in the International Cooperative Pulmonary Embolism Registry (ICOPER). Lancet 1999(9162); 353: 1386-1389.
18. Nakamura M, Fujioka H, Yamada N, et al. Clinical characteristics of acute pulmonary thromboembolism in Japan: results of a multicenter registry in the Japanese Society of Pulmonary Embolism Research. Clin Cardiol 2001(2); 24: 132-138.
19. Goldhaber SZ. Pulmonary embolism. Lancet 2004; 363(9417): 1295-1305.
20. Wells PS, Anderson DR, Rodger M, et al. Derivation of a simple clinical model to categorize patients probability of pulmonary embolism: increasing the models utility with the SimpliRED D-dimer. Thromb Haemost 2000; 83(3): 416-420.
21. Wicki J, Perneger TV, Junod AF, Bounameaux H, Perrier A. Assessing clinical probability of pulmonary embolism in the emergency ward: a simple score. Arch Intern Med. 2001; 161(1): 92-97.
22. Moores LK, Collen JF, Woods KM, Shorr AF. Practical utility of clinical prediction rules for suspected acute pulmonary embolism in a large academic institution. Thromb Res. 2004; 113(1): 1-6.
23. Baxter GM, Duffy P, Partridge E. Colour flow imaging of calf vein thrombosis. Clin Radiol 1992; 46(3): 198-201.
24. Kasper W, Meinertz T, Kersting F, Löllgen H, Limbourg P, Just H. Echocardiography in assessing acute pulmonary hypertension due to pulmonary embolism. Am J Cardiol 1980; 45(3): 567-572.
25. Nixdorff U, Erbel R, Drexler M, Meyer J. Detection of thromboembolus of the right pulmonary artery by transesophageal two dimensional echocardiography. Am J Cardiol 1988; 61(6): 488-489.
26. Lengyel M. Should transesophageal echocardiography become a routine test in patients with suspected pulmonary thromboembolism? Echocardiography 1998; 15(8 pt1): 779-786.
27. Stein PD, Athanasoulis C, Alavi a, et al. Complications and validity of pulmonary angiography in acute pulmonary embolism. Circulation 1992; 85(2): 462-468.
28. Diffin DC, Leyendecker JR, Johnson SP, Zucker RJ, Grebe PJ. Effect of anatomic distribution of pulmonary emboli on interobserver agreement in the interpretation of pulmonary angiography. Am J Roentgenol 1998; 171(4): 1085-1089.
29. Stein PD, Henry JW, Gottschalk A. Reassessment of pulmonary angiography for the diagnosis of pulmonary embolism: relation of interpreter agreement to the order of the involved pulmonary arterial branch. Radiology 1999; 210(3): 689-691.

30. Klingenbeck-Regn K, Schaller S, Flohr T, Ohnesorge B, Kopp AF, Baum U. Subsecond multi-slice computed tomography: basics and applications. Eur J Radiol 1999; 31(2): 110-124.
31. Remy-Jardin M, Remy J, Wattinne L, Giraud F. Central pulmonary thromboembolism: diagnosis with spiral volumetric CT with the single-breath-hold technique - comparison with pulmonary angiography. Radiology 1992; 185(2): 381-387.
32. Remy-Jardin M, Remy J, Deschildre F, et al. Diagnosis of pulmonary embolism with spiral CT: comparison with pulmonary angiography and scintigraphy. Radiology 1996; 200(3): 699-706.
33. van Rossum AB, Pattynama PM, Ton ER, et al. Pulmonary embolism: validation of spiral CT angiography in 149 patients. Radiology 1996; 201(2): 467-470.
34. Mayo JR, Remy-Jardin M, Muller NL, et al. Pulmonary embolism: prospective comparison of spiral CT with ventilation-perfusion scintigraphy. Radiology 1997; 205(2): 447-452.
35. van Rossum AB, Treurniet FE, Kieft GJ, Smith SJ, Schepers-Bok R. Role of spiral volumetric computed tomographic scanning in the assessment of patients with clinical suspicion of pulmonary embolism and an abnormal ventilation/perfusion lung scan. Thorax 1996; 51(1): 23-28.
36. Teigen CL, Maus TP, Sheedy PF, et al. Pulmonary embolism: diagnosis with contrast- enhanced electron-beam CT and comparison with pulmonary angiography. Radiology 1995; 194(2): 313-319.
37. Goodman LR, Curtin JJ, Mewissen MW, et al. Detection of pulmonary embolism in patients with unresolved clinical and scintigraphic diagnosis: helical CT versus angiography. Am J Roentgenol 1995; 164(6): 1369-1374.
38. Velmahos GC, Vassiliu P, Wilcox A, et al. Spiral computed tomography for the diagnosis of pulmonary embolism in critically ill surgical patients: a comparison with pulmonary angiography. Arch Surg. 2001; 136(5): 505-511.
39. Remy-Jardin M, Remy J, Artaud D, Deschildre F, Fribourg M, Beregi JP. Spiral CT of pulmonary embolism: technical considerations and interpretive pitfalls. J Thorac Imaging 1997; 12(2): 103-117.
40. Remy-Jardin M, Remy J, Cauvain O, Petyt L, Wannebroucq J, Beregi JP. Diagnosis of central pulmonary embolism with helical CT: role of two-dimensional multiplanar reformations. Am J Roentgenol 1995; 165(5): 1131-1138.
41. Beigelman C, Chartrand-Lefebvre C, Howarth N, Grenier P. Pitfalls in diagnosis of pulmonary embolism with helical CT angiography. Am J Roentgenol 1998; 171(3): 579-585.
42. Eng J, Krishnan JA, Segal JB, et al. Accuracy of CT in the Diagnosis of Pulmonary Embolism: A Systematic Literature Review. AJR Am J Roentgenol. 2004; 183(6): 1819-27.
43. Rathbun SW, Raskob GE, Whitsett TL. Sensitivity and specificity of helical computed tomography in the diagnosis of pulmonary embolism: a systematic review. Ann Intern Med 2000; 132(3): 227-223.
44. Coche E, Müller NL, Kim K, Wiggs BR, Mayo JR Ancillary findings of acute pulmonary embolism on spiral CT. Radiology 1998; 207(3): 753-758.
45. Sinner WN. Computed tomographic patterns of pulmonary

thromboembolism and infarction. J Comput Assist Tomogr 1978; 2(4): 395-399.
46. Schwickert H, Schweden F, Schild HH, et al. Pulmonary arteries and lung parenchyma in chronic pulmonary embolism: preoperative and postoperative CT findings. Radiology 1994; 191(2): 351-357.
47. Quinn MF, Lundell CJ, Klotz TA, et al. Reliability of selective pulmonary arteriography in the diagnosis of pulmonary embolism. Am J Roentgenol 1987; 149(3): 469-471.
48. Oser RF, Zuckerman DA, Gutierrez FR, Brink JA. Anatomic distribution of pulmonary emboli at pulmonary angiography: implications for cross-sectional imaging. Radiology 1996; 199(1): 31-35.
49. Gurney JW. No fooling around: direct visualization of pulmonary embolism. Radiology 1993; 188(3): 618-619.
50. Dorfman GS, Cronan JJ, Tupper TB, Messersmith RN, Denny DF, Lee CH. Occult pulmonary embolism: a common occurrence in deep venous thrombosis. AJR Am J Roentgenol. 1987;148(2):263-6.
51. Moser KM. Venous thromboembolism. Am Rev Respir Dis 1990; 141(1): 235-249.
52. Baghaie F, Remy-Jardin M, Remy J, Artaud D, Fribourg M, Duhamel A. Diagnosis of peripheral acute pulmonary emboli: optimization of the spiral CT acquisition protocol (abstr). Radiology 1998; 209 (P):299.
53. Remy-Jardin M, Remy J. Spiral CT angiography of the pulmonary circulation. Radiology 1999; 212(3): 615-636.
54. Yankelevitz DF, Shaham D, Shah A, Rademacker J, Henschke CI. Optimization of contrast delivery for pulmonary CT angiography. Clin Imaging 1998; 22(6): 398-403.
55. Thomsen HS, Morcos SK; Contrast Media Safety Committee of European Society of Urogenital Radiology. Management of acute adverse reactions to contrast media. Eur Radiol 2004; 14(3): 476-481.
56. Katayama H, Yamaguchi K, Kozuka T, Takashima T, Seez P, Matsuura K. Adverse reactions to ionic and nonionic contrast media. A report from the Japanese Committee on the Safety of Contrast Media. Radiology 1990; 175(3): 621-628.
57. Thomsen HS, Morcos SK. Contrast media and the kidney: European Society of Urogenital Radiology (ESUR) guidelines. Br J Radiol 2003; 76(908): 513-518.
58. Thomsen HS, Morcos SK; Members of Contrast Media Safety Committee of European Society of Urogenital Radiology (ESUR). In which patients should serum creatinine be measured before iodinated contrast medium administration? Eur Radiol. 2005; 15(4): 749-754.
59. McCartney MM, Gilbert FJ, Murchison LE, Pearson D, McHardy K, Murray AD. Metformin and contrast media--a dangerous combination? Clin Radiol 1999; 54(1): 29-33.
60. Remy-Jardin M, Remy J, Artaud D, Deschildre F, Duhamel A. Peripheral pulmonary arteries: optimization of the spiral CT acquisition protocol. Radiology 1997; 204(1): 157-163.
61. Schlueter FJ, Zuckerman DA, Horesh L, Guttierez FR, Hicks ME, Brinck JA. Digital substraction versus film-screen angiography for detecting acute pulmonary emboli: evaluation in a porcine model. J Vasc Interv Radiol 1997; 8(6): 1015-1024.

62. Coche E, Baile EM, Kim KI, Mayo JR, Wiggs B. Effect of contrast injection rate and site on pulmonary vascular distension. Academic Radiology 1999 Jul; 6(7): 419-425.
63. Baile EM, King GG, Müller NL, et al. Spiral computed tomography is comparable to pulmonary angiography for the diagnosis of pulmonary embolism. Am J Respir Crit Care Med 2000; 161: 1010-1015.
64. Loud PA, Grossman ZD, Klippenstein DL, Ray CE. Combined CT venography and pulmonary angiography: a new diagnostic technique for suspected thromboembolic disease. Am J Roentgenol 1998; 170(4): 951-954.
65. Coche EE, Hamoir XL, Hammer FD, Hainaut P, Goffette PP. Using dual detector helical CT angiography to detect deep venous thrombosis in patients with suspicion of pulmonary embolism: diagnostic value and additional findings. Am J Roentgenol 2001; 176(4): 1035-1039.
66. Loud PA, Katz DS, Bruce DA, Klippenstein DL, Grossman ZD. Deep venous thrombosis with suspected pulmonary embolism: detection with combined CT venography and pulmonary angiography. Radiology 2001; 219(2): 498-502.
67. Abdelmoumene Y, Chevallier P, Barghouth G, et al. Technical innovation. Optimization of multidetector CT venography performed with elastic stockings on patients' lower extremities: A preliminary study of nonthrombosed veins. Am J Roentgenol 2003; 180(4): 1093-1094.
68. Coche EE, Hammer FD, Goffette PP. CT venography performed with elastic stockings. Am J Roentgenol 2004; 182(2): 528; author reply 528-529.
69. Rademaker J, Griesshaber V, Hidajat N, Oestmann JW, Felix R. Combined CT pulmonary angiography and venography for diagnosis of pulmonary embolism and deep vein thrombosis: radiation dose. Rademaker J, Griesshaber V, Hidajat N, Oestmann JW, Felix R. J Thorac Imaging. 2001; 16(4): 297-299.
70. Prokop M. General principles of MDCT. Eur J Radiol 2003; 45 (suppl 1): S4-S10.
71. Simon M, Chiang EE, Boiselle PM. Paddle-wheel multislice helical CT display of pulmonary vessels and other lung structures. Radiol Clin North Am 2003; 41(3): 617-626.
72. Chiang EE, Boiselle PM, Raptopoulos V, Reynolds KF, Rosen MP, Simon M. Detection of pulmonary embolism: comparison of paddlewheel and coronal CT reformations--initial experience. Radiology 2003; 228(2): 577-582.
73. Remy-Jardin M, Tillie-Leblond I, Szapiro D, Ghaye B, Cotte L, Mastora I, Delannoy V, Remy J. CT angiography of pulmonary embolism in patients with underlying respiratory disease: impact of multislice CT on image quality and negative predictive value. Eur Radiol 2002; 12(8): 1971-1978.
74. Coche E, Pawlak S, Dechambre S, Maldague B. Peripheral pulmonary arteries: identification at multislice spiral CT with 3D reconstruction. Eur Radiol 2003; 13(4): 815-822.
75. Ghaye B, Szapiro D, Mastora I, et al. Peripheral pulmonary arteries: how far in the lung does multi-detector row spiral CT allow analysis? Radiology 2001; 219(3): 629-636.
76. Patel S, Kazerooni EA, Cascade PN. Pulmonary embolism: optimization of

small pulmonary artery visualization at multi-detector row CT. Radiology 2003; 227(2): 455-460.
77. Raptopoulos V, Boiselle PM. Multi-detector row spiral CT pulmonary angiography: comparison with single-detector row spiral CT. Radiology 2001; 221(3): 606-613.
78. Qanadli SD, Hajjam ME, Mesurolle B, et al. Pulmonary embolism detection: prospective evaluation of dual-section helical CT versus selective pulmonary arteriography in 157 patients. Radiology. 2000; 217(2): 447-455.
79. Coche E, Verschuren F, Keyeux A, et al. Diagnosis of acute pulmonary embolism in outpatients: comparison of thin-collimation multi-detector row spiral CT and planar ventilation-perfusion scintigraphy. Radiology 2003; 229(3): 757-765.
80. Winer-Muram HT, Rydberg J, Johnson MS, et al. Suspected acute pulmonary embolism: evaluation with multi-detector row CT versus digital subtraction pulmonary arteriography. Radiology 2004; 233(3): 806-815.
81. Holbert JM, Costello P, Federle MP. Role of spiral computed tomography in the diagnosis of pulmonary embolism in the emergency department. Ann Emerg Med 1999; 33(5): 520-528.
82. Drucker EA, Rivitz SM, Shepard JA, et al. Acute pulmonary embolism: assessment of helical CT for diagnosis. Radiology 1998; 209(1): 235-241.
83. Kim KI, Muller NL, Mayo JR. Clinically suspected pulmonary embolism: utility of spiral CT. Radiology 1999; 210(3): 693-697.
84. Schoepf UJ, Bruening RD, Hong C, et al. Multislice helical CT of focal and diffuse lung disease: comprehensive diagnosis with reconstruction of contiguous and high-resolution CT sections from a single thin-collimation scan. Am J Roentgenol 2001; 177(1): 179-184.
85. Schoepf UJ, Holznecht N, Helmberger TK, et al. Subsegmental pulmonary emboli: improved detection with thin-collimation multi-detector rows spiral CT. Radiology 2002; 222(2): 483-490.
86. Coche E, Greesens B, Dechambre S, Goncette L, Verschuren F. Embolies périphériques au CT scanner multidétecteur: prévalence, clinique et implications techniques. Abstr Journal de Radiologie (2004).
87. Ginsberg MS, King V, Panicek DM. Comparison of interpretations of CT angiograms in the evaluation of suspected pulmonary embolism by on-call radiology fellows and subsequently by radiology faculty. AJR Am J Roentgenol 2004; 182(1): 61-66.
88. Perrier A, Bounameaux H. Cost-effective diagnosis of deep vein thrombosis and pulmonary embolism. Thromb Haemost 2001; 86(1): 475-487.
89. Perrier A, Bounameaux H. Diagnosis of pulmonary embolism in outpatients by sequential noninvasive tools. Semin Thromb Hemost 2001; 27(1): 25-32.
90. Bounameaux H, de Moerloose P, Perrier A, Miron MJ. D-dimer testing in suspected venous thromboembolism: an update. QJM1997;90(7):437-442.
91. Anderson DR, Wells PS, Stiell I, et al. Management of patients with suspected deep vein thrombosis in the emergency department: combining use of a clinical diagnosis model with D-dimer testing. J Emerg Med 2000; 19(3): 225-230.
92. Oger E, Leroyer C, Bressollette L, et al. Evaluation of a new, rapid, and

quantitative D-Dimer test in patients with suspected pulmonary embolism. Am J Respir Crit Care Med 1998; 158(1): 65-70.
93. Duet M, Benelhadj S, Kedra W, et al. A new quantitative D-dimer assay appropriate in emergency: reliability of the assay for pulmonary embolism exclusion diagnosis. Thromb Res 1998; 91(1): 1-5.
94. Abcarian PW, Sweet JD, Watabe JT, Yoon HC. Role of a quantitative D-dimer assay in determining the need for CT angiography of acute pulmonary embolism. AJR Am J Roentgenol 2004; 182(6): 1377-1381.
95. Schoepf UJ, Costello P. CT angiography for diagnosis of pulmonary embolism: state of the art. Radiology. 2004; 230(2): 329-337.
96. Resten A, Mausoleo F, Valero M, Musset D. Comparison of doses for pulmonary embolism detection with helical CT and pulmonary angiography. Eur Radiol 2003; 13(7): 1515-1521.
97. Kuiper JW, Geleijns J, Matheijssen NA, Teeuwisse W, Pattynama PM. Radiation exposure of multi-row detector spiral computed tomography of the pulmonary arteries: comparison with digital subtraction pulmonary angiography. Eur Radiol 2003; 13(7): 1496-1500.
98. Kalender WA, Wolf H, Suess C, Gies M, Greess H, Bautz WA. Dose reduction in CT by on-line tube current control: principles and validation on phantoms and cadavers. Eur Radiol 1999; 9(2): 323-328.
99. Gies M, Kalender WA, Wolf H, Suess C. Dose reduction in CT by anatomically adapted tube current modulation. I. Simulation studies. Med Phys 1999; 26(11): 2235-2247.
100. Tack D, De Maertelaer V, Gevenois PA. Dose reduction in multidetector CT using attenuation-based online tube current modulation. AJR Am J Roentgenol 2003; 181(2): 331-334.
101. Mastora I, Remy-Jardin M, Delannoy V, et al. Multi-detector row spiral CT angiography of the thoracic outlet: dose reduction with anatomically adapted online tube current modulation and preset dose savings. Radiology 2004; 230(1): 116-124.
102. Nagels HD. Factors influencing patient dose in CT. In Nagel HD, ed, Radiation exposure in Computed Tomography. 2nd ed. Hamburg, Germany, European Coordination Committee of the Radiological and Electromedical Industries 2000; 25-44.
103. Kalra MK, Maher MM, Toth TL, et al. Strategies for CT radiation dose optimization. Radiology 2004; 230(3): 619-628.
104. Hamberg LM, Rhea JT, Hunter GJ, Thrall JH. Multidetector-row CT: radiation dose characteristics. Radiology 2003; 226(3): 762-772.
105. Coche E, Vlassenbroek A, Denis JM, Octave-Prignot M, Van Beers B, Vynckier S. Radiation doses with multi-slice CT: comparison of dual, quad and 16 slices CT. Abstr Eur Radiol 2004.
106. Tack D, De Maertelaer V, Petit W, et al. Comparisons of Standard-Dose and Simulated Low-Dose Multi-Detector-Row CT Pulmonary Angiography. Radiology (in press).
107. Schuster ME, Fishman JE, Copeland JF, Hatabu H, Boiselle PM. Pulmonary embolism in pregnant patients: a survey of practices and policies for CT pulmonary angiography. AJR Am J Roentgenol 2003; 181(6): 1495-1498.
108. Winer-Muram HT, Boone JM, Brown HL, Jennings SG, Mabie WC, Lombardo GT. Pulmonary embolism in pregnant patients: fetal radiation

dose with helical CT. Radiology 2002; 224(2): 487-492.
109. Fleishmann D. Use of high-concentration contrast media in multiple-detector row CT: principles and rationale. Eur Radiol 2003; 13: M14-M20.
110. Kirchner J, Kickuth R, Laufer U, Noack M, Liermann D. Optimized enhancement in helical CT: experience with a real time bolus tracking system in 628 patients. Clinical radiology 2000; 55(5): 368-373.
111. Dorio PJ, Lee FT Jr, Henseler KP, et al. Using a saline chaser to decrease contrast media in abdominal CT. Am J Roentgenol 2003; 180(4): 929-934.
112. Bae KT, Heiken JP, Brink JA. Aortic and hepatic contrast medium enhancement at CT. Part I. Prediction with a computer model. Radiology 1998; 207(3): 647-655.
113. Coche E, Hammer FD, Goffette P. Demonstration of pulmonary embolism with dynamic gadolinium-enhanced spiral CT. Eur Radiol 2001; 11(11): 2306-2309.
114. Bloem JL, Wondergem J. Gd-DTPA as a contrast agent in CT. Radiology 1989; 171(2): 578-579.
115. Gierada DS, Bae KT. Gadolinium as CT contrast agent: assessment in a porcine model. Radiology 1999; 210(3): 829-834
116. Quinn AD, O'Hare NJ, Wallis FJ, Wilson GF. Gd-DTPA: an alternative contrast medium for CT. J Comput Assist Tomogr 1994; 18(4): 634-636.
117. Remy-Jardin M, Bahépar J, Ertzbischoff O, Dequiedt P, Duhamel A, Remy J . Sixteen-slice multidetector CT angiography of the pulmonary circulation using Gadolinium-based contrast agents: prospective evaluation in 54 patients (Abstr.) RSNA 2004, 607.
118. Bae KT, McDermott R, Gierada DS, et al. Gadolinium-enhanced computed tomography angiography in multi-detector row computed tomography: initial observations. Acad Radiol 2004; 11(1): 61-68.
119. Tourassi GD, Frederick ED, Floyd CE Jr, Coleman RE. Multifractal texture analysis of perfusion lung scans as a potential diagnostic tool for acute pulmonary embolism. Comput Biol Med 2001; 31(1): 15-25.
120. Schoepf UJ, Das M, Schneider AC et al. Computer aided detection (CAD) of segmental and subsegmental pulmonary emboli on 1-mm multidetector-row CT (MDCT) studies. (Abstr.) RSNA 2002: 384-385.
121. Masutani Y, MacMahon H, Doi K. Computerized detection of pulmonary embolism in spiral CT angiography based on volumetric image analysis. IEEE Trans Med Imaging 2002; 21(12): 1517-1523.
122. Schoepf UJ, MD, Bruening R, MD, Konschitzky H, et al. Pulmonary embolism: comprehensive diagnosis by using electron-beam CT for detection of emboli and assessment of pulmonary blood flow. Radiology 2000; 217(3): 693-700.
123. Bankier AA, Janata K, Fleischmann D, et al. Severity assessment of acute pulmonary embolism with spiral CT: evaluation of two modified angiographic scores and comparison with clinical data. J Thorac Imaging 1997; 12(2): 150-158.
124. Qanadli SD, El Hajjam M, Vieillard-Baron A, et al. New CT index to quantify arterial obstruction in pulmonary embolism: comparison with angiographic index and echocardiography. Am J Roentgenol 2001; 176(6): 1415-1420.
125. Mastora I, Remy-Jardin M, Masson P, et al. Severity of acute

pulmonary embolism: evaluation of a new spiral CT angiographic score in correlation with echocardiographic data. Eur Radiol 2003; 13(1): 29-35.
126. Wu AS, Pezzullo JA, Cronan JJ, Hou DD, Mayo-Smith WW. CT pulmonary angiography: quantification of pulmonary embolus as a predictor of patient outcome--initial experience. Radiology 2004; 230(3): 831-835.
127. Carson JL, Kelley MA, Duff A, et al. The clinical course of pulmonary embolism. N Engl J Med 1992; 326(19): 1240-1245.
128. Ribeiro A, Lindmarker P, Juhlin-Dannfelt A, Johnsson H, Jorfeldt L. Echocardiography Doppler in pulmonary embolism: right ventricular dysfunction as a predictor of mortality rate. Am Heart J 1997; 134(3): 479-487.
129. Kasper W, Konstantinides S, Geibel A, et al. Prognostic significance of right ventricle afterload stress detected by echocardiography in patients with clinically suspected pulmonary embolism. Heart 1997; 77(4): 346-349.
130. Contractor S, Maldjian PD, Sharma VK, Gor DM. Role of helical CT in detecting right ventricular dysfunction secondary to acute pulmonary embolism. J Comput Assist Tomogr 2002; 26(4): 587-591.
131. Quiroz R, Kucher N, Schoepf UJ, et al. Right ventricular enlargement on chest computed tomography: prognostic role in acute pulmonary embolism. Circulation 2004; 109(20): 2401-2404.
132. Flohr T, Prokop M, Becker C, et al. A retrospectively ECG-gated multislice spiral CT scan and reconstruction technique with suppression of heart pulsation artifacts for cardio-thoracic imaging with extended volume coverage. Eur Radiol 2002; 12(6): 1497-1503.
133. Juergens KU, Grude M, Maintz D, et al. Multi-detector row CT of left ventricular function with dedicated analysis software versus MR imaging: initial experience. Radiology 2004; 230(2): 403-410.
134. Coche E, Vlassenbroek A, Roelants V, et al. Evaluation of biventricular ejection fraction with ECG-gated 16-slice CT: preliminary findings in acute pulmonary embolism in comparison with radionuclide ventriculography. Eur Radiol 2005 (in press).
135. Coche E, de Crombrugghe R, Vlassenbroek A. Right ventricular function measured during ECG-gated MSCT of the whole chest: Intra-and inter-observer variability. Eur radiol 2005. Abstr.
136. Coche E, Verschuren F, Hainaut P, Goncette L. Pulmonary embolism findings on chest radiographs and multislice spiral CT. Eur Radiol 2004; 14(7): 1241-1248.
137. Kalender WA. The use of flat-panel detectors for CT imaging. Radiologe 2003; 43(5): 379-387.
138. Ning R, Chen B, Yu R, Conover D, Tang X, Ning Y. Flat panel detector-based cone-beam volume CT angiography imaging: system evaluation. IEEE Trans Med Imaging 2000; 19(9): 949-963.
139. Jaffray DA, Siewerdsen JH. Cone-beam computed tomography with a flat-panel imager: initial performance characterization. Med Phys 2000; 27(6): 1311-1323.
140. Salovic D, Humblet Y, Coche E. Diagnosis of pulmonary embolism with 16 slice-CT. JBR–BTR 2003; 86(2): 113.
141. Coche E, Verschuren F, Kefer J. Acute coronary occlusion revealed by ECG-gated 16-slice CT of the whole chest. European Heart Journal 2005

(In press).
142. Kasper W, Meinertz T, Henkel B, Eissner D, Hahn K, Hofmann T, Zeiher A, Just H. Echocardiographic findings in patients with proved pulmonary embolism. Am Heart J. 1986; 112(6): 1284-90.

9.2. Personal contribution :

1. **Coche E**, Goncette L, Pringot J. Spiral CT in pulmonary embolism. JBR-BJR 1998; 81(4): 199-203.
2. **Coche E**, Müller NL, Kim KI, Wiggs BR, Mayo JR. Acute pulmonary embolism: ancillary findings at spiral CT. Radiology 1998; 207: 753-758.
3. **Coche E,** Baile EM, Wiggs BR, Kim KI, Mayo JR. Effect of site and rate of contrast material injection on pulmonary vascular distension. Academic Radiology 1999; 6(7): 419-425.
4. Baile EM, King GG, Müller NL, D'Yachkova Y, **Coche E**, Paré PD, Mayo JR. Spiral computed tomography is comparable to angiography for the diagnosis of pulmonary embolism. Am J Respir Crit Care Med 2000; 161: 1010-1015.
5. **Coche E**, Hamoir XL, Hammer FD, Hainaut P, Goffette PP. Using dual-detector helical CT angiography to detect deep venous thrombosis in patients with suspicion of pulmonary embolism: diagnostic value and additional findings. AJR Am J Roentgenology 2001; 176(4): 1035-1039.
6. **Coche E,** Hammer F, Goffette P. CT venography performed with elastic stockings. Letter AJR Am J Roentgenol 2004; 182(2): 528; author's reply 528-529.
7. **Coche E,** Pawlak S, Dechambre S, Maldague B. Peripheral pulmonary arteries: identification at multi-slice spiral CT with 3D reconstruction. Eur Radiol 2003; 13(4): 815-822.
8. **Coche E,** Verschuren F, Keyeux A, Goffette P, Goncette L, Hainaut P, Hammer F, Lavenne E, Zech F, Meert P, Reynaert M. Diagnosis of acute pulmonary embolism in outpatients: comparison of thin-collimation multi-detector row spiral CT and planar ventilation-perfusion scintigraphy. Radiology 2003; 229(3): 757-765.
9. Reinartz P, Nowak B, Weiss C, Buell U. Acute pulmonary embolism: thin-collimation spiral CT versus planar ventilation-perfusion scintigraphy. **Coche E**, V Roelants, Keyeux A, Verschuren F, Zech F. Reply letter. Radiology. 2004; 232(2): 621
10. **Coche E,** Vynckier S, Octave-Prignot M. Radiation exposure during diagnostic work-up of pulmonary embolism: a comparative study with 4, 16-slices CT scanners and digitalized pulmonary angiography using an anthropomorphic phantom. Submitted to Radiology (in process).
11. **Coche E,** Hammer FD, Goffette P. Demonstration of pulmonary embolism with gadolinium-enhanced spiral CT. Eur Radiol 2001; 11(11): 2306-2309.
12. **Coche E**, Vlassenbroek A, Roelants V, D'Hoore W, Verschuren F, Goncette L, Maldague B. Evaluation of biventricular ejection fraction with ECG-gated 16-slice CT: pulmonary findings in acute pulmonary embolism in comparison with radionuclide ventriculography. Eur Radiol 2005, in press.

13. **Coche E,** Verschuren F, Hainaut P, Goncette L. Pulmonary embolism findings on chest radiographs and multislice spiral CT. Eur Radiol 2004; 14(7): 1241-8.